United States
Environmental Protection
Agency

Industrial Environmental Research
Laboratory
Research Triangle Park NC 27711

EPA-600/7-79-238
November 1979

EPA

EPA/IERL-RTP Pilot Electrostatic Precipitator - Selected Experiments, 1978

Interagency Energy/Environment R&D Program Report

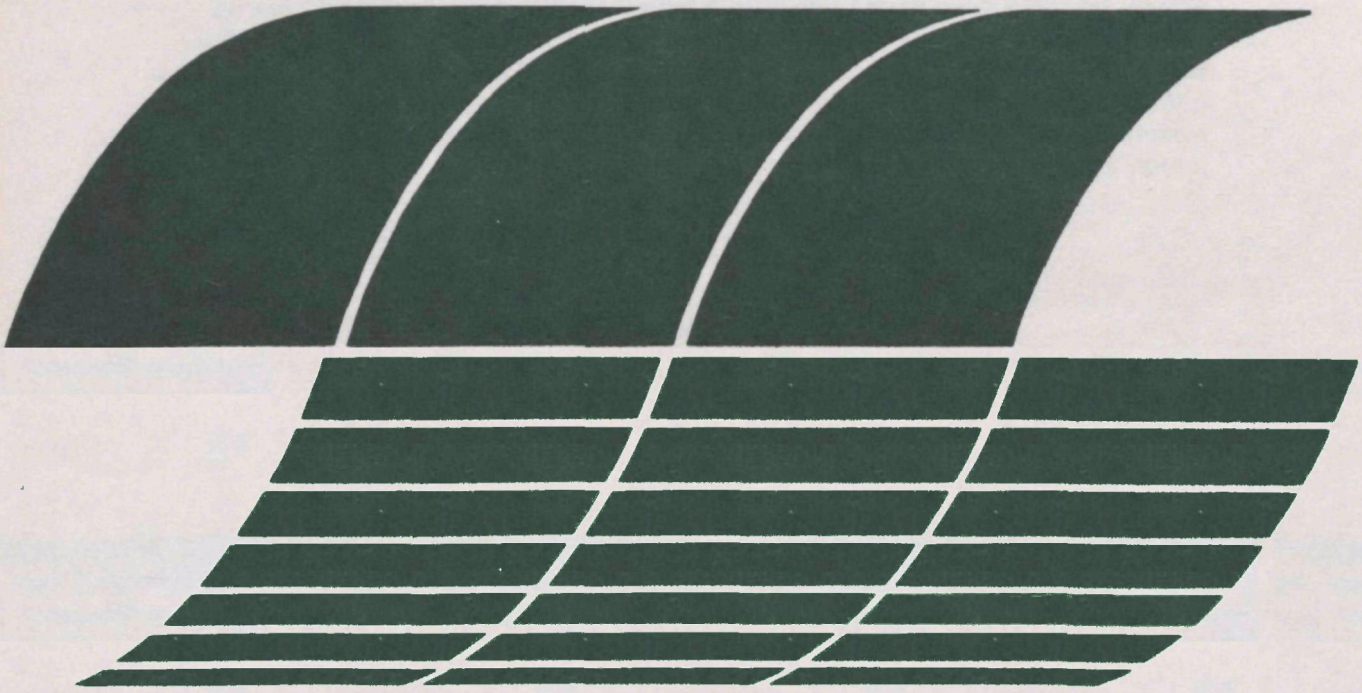

RESEARCH REPORTING SERIES

Research reports of the Office of Research and Development, U.S. Environmental Protection Agency, have been grouped into nine series. These nine broad categories were established to facilitate further development and application of environmental technology. Elimination of traditional grouping was consciously planned to foster technology transfer and a maximum interface in related fields. The nine series are:

1. Environmental Health Effects Research
2. Environmental Protection Technology
3. Ecological Research
4. Environmental Monitoring
5. Socioeconomic Environmental Studies
6. Scientific and Technical Assessment Reports (STAR)
7. Interagency Energy-Environment Research and Development
8. "Special" Reports
9. Miscellaneous Reports

This report has been assigned to the INTERAGENCY ENERGY-ENVIRONMENT RESEARCH AND DEVELOPMENT series. Reports in this series result from the effort funded under the 17-agency Federal Energy/Environment Research and Development Program. These studies relate to EPA's mission to protect the public health and welfare from adverse effects of pollutants associated with energy systems. The goal of the Program is to assure the rapid development of domestic energy supplies in an environmentally-compatible manner by providing the necessary environmental data and control technology. Investigations include analyses of the transport of energy-related pollutants and their health and ecological effects; assessments of, and development of, control technologies for energy systems; and integrated assessments of a wide range of energy-related environmental issues.

EPA REVIEW NOTICE

This report has been reviewed by the participating Federal Agencies, and approved for publication. Mention of trade names or commercial products does not constitute endorsement or recommendation for use.

This document is available to the public through the National Technical Information Service, Springfield, Virginia 22161.

EPA-600/7-79-238

November 1979

EPA/IERL-RTP Pilot Electrostatic Precipitator – Selected Experiments, 1978

by

D.W. VanOsdell (RTI), L.E. Sparks, G.H. Ramsey,
and B.E. Daniel

Industrial Environmental Research Laboratory
Office of Environmental Engineering and Technology
Research Triangle Park, NC 27711

Program Element No. EHE624A

U.S. ENVIRONMENTAL PROTECTION AGENCY
Office of Research and Development
Washington, DC 20460

ABSTRACT

This report deals with experiments run on a pilot-scale electrostatic precipitator located at IERL-RTP. The precipitator is a dedicated experimental tool which is operated for experiments originated and designed both in-house and by EPA contractors.

Five distinct test series conducted between March and October 1978 are described in this report. The areas of study were precharger operation, precipitator operating characteristics, reentrainment, parameter variation with position within precipitator, and effects of humidity.

The results of the precharger test series were inconclusive; removal efficiency was 10 to 20 percent better with the precharger for most size ranges, but its operation was erratic in this preliminary test. The reentrainment test demonstrated that sparking produced more and larger particulate than other reentrainment mechanisms. No pattern of size distribution change was established.

The study of flow, mass, and particle size as a function of sample probe position showed that parameter variations do exist. The data collected was not sufficient to fully establish the differences.

The study of the effects of humidity on collection efficiency demonstrated that increased moisture had a strong impact on improved performance. The moisture lowers the particulate resistivity, allowing increased electrical fields. Efficiency correlated well with voltage in the form:

$$P = 6.59 \times 10^{8} V^{-5.46}$$

where P = penetration, %

V = voltage, kV.

The correlation coefficient, r^2, was 0.97.

TABLE OF CONTENTS

LIST OF FIGURES

LIST OF TABLES

ACKNOWLEDGEMENT

The assistance of coauthor VanOsdell is acknowledged. His contribution was funded under U.S. Environmental Protection Agency Grant No. R805897 with Research Triangle Institute.

1.0 SUMMARY

This report deals with experiments run on a pilot-scale electrostatic precipitator (ESP) located at IERL-RTP. The ESP is a dedicated experimental tool which is operated for experiments originated and designed both in-house and by EPA contractors. Experiments designed by contractors are generally reported separately; work which originated in-house and was completed between March and October 1978 is included in this report.

This experimental work falls into five categories, each described in a separate section of the report. The first group of runs were the preliminary precharger experiments, March 1978. An experimental precharger test section designed by Southern Research Institute was installed in the ESP and operated for 3 days. The test was designed more as a trial run for the precharger concept than as a complete experimental investigation. The results were inconclusive, although the precharger appeared to improve collection. A second-generation precharger has since been installed permanently on the ESP.

The second data set was concerned with general characterization of ESP operation, with particular attention to ESP efficiency. The data indicate that the ESP electrical conditions control efficiency and that back-corona and sparking control electrical conditions.

A series of runs were made in April 1978 to study reentrainment effects. Only 2 days were devoted to the study, and scatter makes the data difficult to interpret. Rapping appears to generate a larger particle size distribution than that which is generated by simple viscous reentrainment.

The effect of sample location within the ESP on the values of some experimental variables was investigated with several runs in May and June 1978. The velocity profile across the ESP is relatively flat except within 2 cm or so of the walls. Mass loading increases slightly toward the wall, and there is an increase in the mean diameter as the probe is moved closer to the wall.

The last series of runs included in this report is a 10 run set concluded in October 1978. The humidity of the carrier gas was changed by steam injection, and its effect on ESP operation studied. The data indicate that the increased humidity improves performance and that the improved performance is due to improved electrical characteristics (reduced resistivity) of the dust. The overall penetration correlated very well with ESP voltage. The best fit was obtained with a power function: penetration was inversely proportional to voltage to the 5.45 power.

2.0 IERL-RTP PILOT-SCALE ESP

2.1 INTRODUCTION

The IERL-RTP pilot-scale ESP was constructed as a dedicated experimental tool for the investigation of factors which influence ESP operation. The performance of an ESP can be described in terms of inputs (dust, gas rate and conditions, electrical parameters, etc) and its functional characteristics (number of sections, flow channels, plate areas, baffling, etc.). The complexity of the total ESP system, the cost of experimentation, and the difficulty of controlling variables preclude careful single-variable study in an industrial ESP. The pilot-scale ESP was built to overcome these difficulties. The pilot unit has the flexibility to allow the study of the effects of individual functional groups on ESP performance. To achieve this flexibility, the pilot-scale ESP features:

1. readily adjustable plate spacing,
2. readily adjustable wire number, spacing, and type,
3. temperature control from ambient to 350°C,
4. gas velocities from 0.3 to 6.0 m/sec,
5. sampling ports between each pair of sections, and
6. extensive electrical monitoring equipment.

2.2 DESIGN FEATURES

Physical Characteristics

The pilot-scale ESP consists of an inlet section, transition/test section, and four dust collection sections followed by ducting which leads to an exhaust blower and stack. In cross section the ESP is roughly 2 m high by 1 m wide overall, and the overall length is about 15 m. The ESP was designed and installed by Denver Research Institute* and was fabricated by Stainless Equipment Company**. Figure 2.1 is an elevation of the ESP, roughly to scale.

The inlet section of the ESP is about 4 m long, with the same cross section as the remainder of the unit. Ambient air is drawn directly into the ESP through a coarse screen. The burners used for temperature control and the aerosol and steam injection ports are located in this section.

---

*Denver Research Institute, University of Denver, Denver, Colorado 80210.

**Stainless Equipment Company, 2829 S. Santa Fe Drive, Englewood, Colorado 80110.

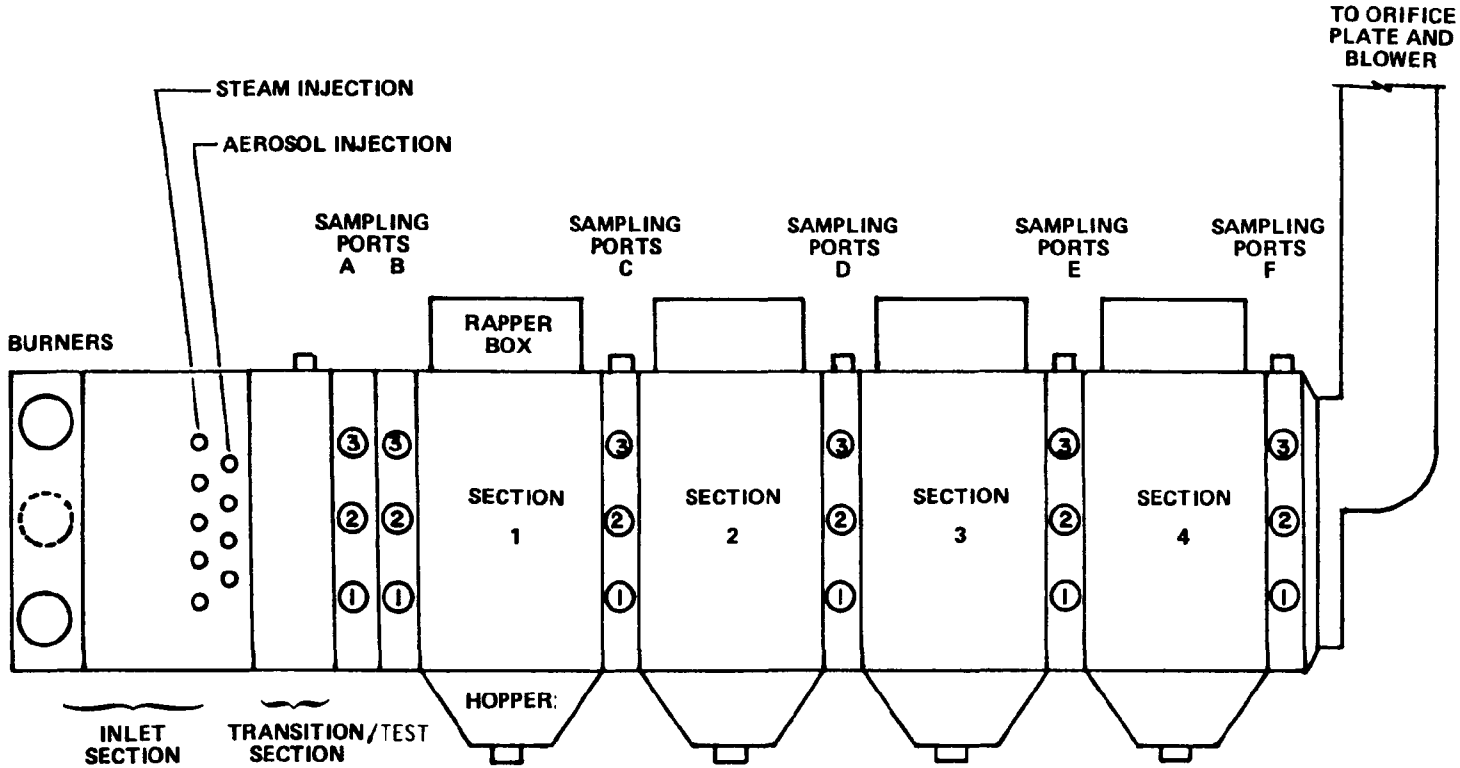

Figure 2.1 Diagram of pilot-scale ESP.

The transition/test section normally serves only to allow flow development as the gas nears the sampling ports. This section can be removed to allow insertion of test modules of various types.

There are four identical dust collection sections in the direction of flow. There is only one lane for gas flow; the collection plates are 1.22 m square and parallel. Plate-to-plate spacing can be readily varied from 12.7 to 38 cm. The specific collector area (SCA) of the ESP is 28 $m^2/m^3/sec$ at a plate spacing of 23 cm and a gas velocity of 1.5 m/sec. The discharge electrodes are wires hung from an overhead support; they can easily be moved to change the number of wires, wire-to-wire spacing, and wire type. Access to the wires is through the hinged side of the pilot unit.

Gas Flow and Conditioning

The carrier gas in the ESP is ambient air; the air can be conditioned by heating, steam injection, gas injection, and aerosol injection. Flow distribution has been measured within the ESP and is relatively uniform. Although plate spacing is variable in the dust collection sections, the inlet and outlet duct sizes are fixed. Transition plates before the first section and after the last reduce the abruptness of the change in cross section. These plates do not ensure a totally uniform flow field, particularly at the inlet of the first dust collection section at narrow plate spacing. As might be expected, the flow rate is highest toward the center of the flow lane (Table 2.1), with a slight drop at the vertical centerline, probably due to the wires. The coefficient of variation (CV) of the flow rate is used as a measure of smoothness of flow. The narrowest plate spacing has the highest variation for two reasons: the transition is sharpest, and the velocity traverse includes more points close to the wall because the traverse point spacing is reduced at close plate spacings.

Table 2.1. Flow Distributions at Different Plate Spacings

Volumetric Flow Rate	Plate Spacings 38 cm Avg. Velocity, m/sec	CV, %	25 cm Avg. Velocity, m/sec	CV, %	13 cm Avg. Velocity, m/sec	CV, %
Low	38.4	46	65.6	37	31.4	56
Medium	100.7	45	98.5	43	78.4	66
High	188.0	49	182.0	58	138.0	58
Range of CV in Each Section	15-25%		0.10-0.20 10-20%		0.05-0.38 5-38%	

Baffling is used extensively throughout the ESP to reduce the extent of sneakage. Sneakage is estimated based on flow measurements made in the hoppers, between sections, and through the top of the ESP. It is estimated that sneakage through the top of the impactor sections amounts to 7 to 9 percent of the gas flow and that sneakage through the hoppers amounts to about 3 percent of the gas.

Temperature of the ESP is controlled by two heating systems. The primary system consists of three 125,000 kcal/hr LPG burners. The temperature of the ESP can be controlled to between ambient and 350°C. The second heating system consists of electric strip heaters in the dust collection sections which are designed to make up heat losses down the length of the ESP.

The gas burners are controlled by a thermocouple in the inlet section. This control thermocouple maintains the temperature within ±5°C of the setpoint. There are temperature gradients both vertically

within each section and down the length of the ESP (in spite of the supplementary heaters). At various burner rates and with different burners, the vertical temperature gradient is 30 to 45°C in the inlet section. Vertical gradients have not been determined in the dust collection sections. Temperature drop down the length of the ESP amounts to about 10°C per section even with the supplementary heaters.

The ESP can be heated to its maximum operating temperature in about an hour with the three main burners on full. After attaining the operating range, the temperature can be maintained with only one burner.

Humidity Control

Humidity is controlled (above ambient water loadings) by steam injection. An LPG-fired boiler generates the steam, which is injected under pressure. The most commonly used pressure has been 378 kPa absolute. Steam flow rate is not monitored.

Aerosol Generation/Dispersion

Aerosol can be injected into the ESP at five ports just upstream of the temperature controlling thermocouple. The dust used to date has been flyash from Illinois coal burned at a Detroit Edison Co. power plant. The flyash to be reentrained is delivered to a hopper by an adjustable screw feeder. Low-cost, commercial sandblast guns draw on the hopper and inject the flyash into the ESP. A cyclone is installed in the line between the feeder hopper and the sandblast guns to remove the largest particles and reduce particle fallout in the inlet region of the ESP. Air pressures of 2 to 8 MPa (10 to 60 psig) have been used to drive the aerosol injection; at 3 MPa (15 psig), an air flow of about 15.5 ℓ/sec (10 scfm) is required. The dust from the sandblast guns is directed into the air flow in the ESP to maximize its dispersal.

Operation has been studied with two and three sandblast guns. Two-gun operation gives satisfactory results; the vertical mass distribution at section A was determined to have a coefficient of variation of 0.14. Measurements of the horizontal distribution at the middle port of section A had a coefficient of variation of 0.12 for a 25-cm plate spacing and 0.04 for a 38-cm plate spacing, indicating that the dust is well distributed across the duct.

Electrical System

The four dust collection sections are identical: the description of one will suffice for all. For safety reasons, numerous electrical and mechanical interlocks remove all voltages from the ESP sections when the integrity of the machine is breached. These interlocks are not included in the description below.

Transformer/Rectifier Sets--Each power supply is a Hipotronics* T8100-10, capable of delivering 0-100 kV dc at 10 mA. Rectification is by solid-state diodes in either half- or full-wave bridge configurations. The output of the power supply can be filtered with a 0.01 μF capacitor, or the capacitor can be disconnected. The power supply contains an internal voltage divider resistor for measuring output voltage; the return connection of the power supply is used for measuring direct current.

The primary voltage is changed from zero to 208 V ac by a variable transformer. Current limiting devices between the transformer output and power supply input protect the power supply during sparkover. These devices comprise a high inductance choke in series with high wattage resistors which are switchable in values of zero, 5, 10, and 20 ohms. When measuring high operating voltages and currents, the series resistance must be lowered.

Corona Frame and Collecting Plates--High voltage is supplied to the corona wires through the corona frame, which is a 5-cm diameter pipe 1.25 m long, with closed, rounded ends. It is suspended at each end from rods which pass up into the rapper box. These support rods are enclosed in cylindrical metal tunnels and terminate at the top in large corona balls (about 20 cm in diameter). The balls rest on insulating plates across the top of each tunnel, which serve as both electrical insulators and seals to prevent infiltration.

The corona frame can support weighted wires in a variety of configurations. Over the 1.3-m length of the high-voltage frame, 48 wire receptacles are spaced 2.5 cm apart, allowing from 2 to 10 or 12 wires per section to be set up quickly and easily. The receptacles are cone-shaped depressions which match cones swaged to the upper ends of the corona wires; the wire

*Hipotronics, Inc., Drawer A, Brewster, New York 10590.

cones hang in the receptacles and support the weight of the wire. For the work included in this report, the wires were a standard 0.32 cm (0.125 inch) in diameter.

Each collecting plate has an effective area of 1.5 m^2, and each is hung from a support that travels on a rotating threaded rod. When the rod is turned, using an external crank, the supports travel toward or away from one another to vary the plate spacing. The motion is symmetrical with respect to the corona wires.

An air-operated rapper above each plate moves with it. The air lines, flexible enough to accommodate the plate motion, also electrically isolate the rapper from the system ground. Rapper operation is now automatic, controlled by a card-programmable timer. For much of the work reported here, operation was manual.

The collector plate is electrically isolated from its support frame by strips of a mica-based material. The entire plate area opposite the corona wires is electrically connected, separate from the frame and baffles at the sides and bottom of the frame. A lead from the collector plate in each electrical section returns to the power supply ground through a sensing resistor, permitting direct measurement of plate current from both collectors in each section. Separate leads from each plate are connected externally for this measurement; however, the current to each plate can be measured using each lead individually.

Measurement System--The measurement system of the pilot-scale ESP consists of transducers, signal conditioning preamplifiers, digitizing and display circuits, and a hard-copy printer. Outputs from the voltage transducers range from zero to 1 V full-scale; from the current transducers, from zero to 5.0 V full-scale; from the temperature tranducers, zero to 100 mV full-scale; and from the pressure transducer for the flow measurement, zero to 10 V full-scale.

Voltage and current signals can be viewed directly on a dual-channel oscilloscope, one section at a time, selected by switches. For measurement, all signals are filtered and amplified or attenuated between zero and 100 mV by a separate preamplifier for each signal channel. The filtering removes noise pulses and power-line-induced pickup from the conditioned signals and helps protect the preamplifier inputs from surges during sparking.

Preamplifier outputs are sampled in succession at the rate of about twice a second by a multiplexer. The multiplexer output is fed to an analog-to-digital converter (ADC). The ADC produces a three-digit representation of the signal presented to it by the multiplexer and puts that representation on a data bus. The data on the bus is put into the proper display unit by an unlatching pulse fed to that unit. The unlatching pulses are directed by a digital multiplexer that operates in the same sequence as the signal multiplexer.

In normal operation, each display is updated approximately twice a second. The multiplexer can be locked onto any channel for more rapid updating.

The same data bus feeds a parallel-to-serial converter whose output goes to a standard 80-character thermal line printer. The data are punctuated and formatted by characters stored in a read-only memory (ROM). A heading that can be printed manually is also stored in the ROM. Data printing can be initiated manually at any time or can be performed automatically at 1- or 10-minute intervals, controlled by a digital clock. The clock operates continuously from the power line, providing initiation pulses and time of data collection for each line on the printer. A manual keyboard on the printer can be used to enter information about the data being printed.

Voltage/Current Characteristics--The variation of corona current (I) with applied voltage (V) has been measured for the pilot-scale ESP under various conditions. As a base case, the VI curve for the ESP with clean plates and wires and with careful alignment of all components is presented in Figure 2.2. The VI curves for sections 1, 2, and 3 are all essentially coincident with each other and with theoretical predictions. The section 4 curve was different because of the different plate-to-plate spacing, but it too is consistent with theoretical predictions. Dirty plate VI curves tend to show measurable current before theory would predict corona.

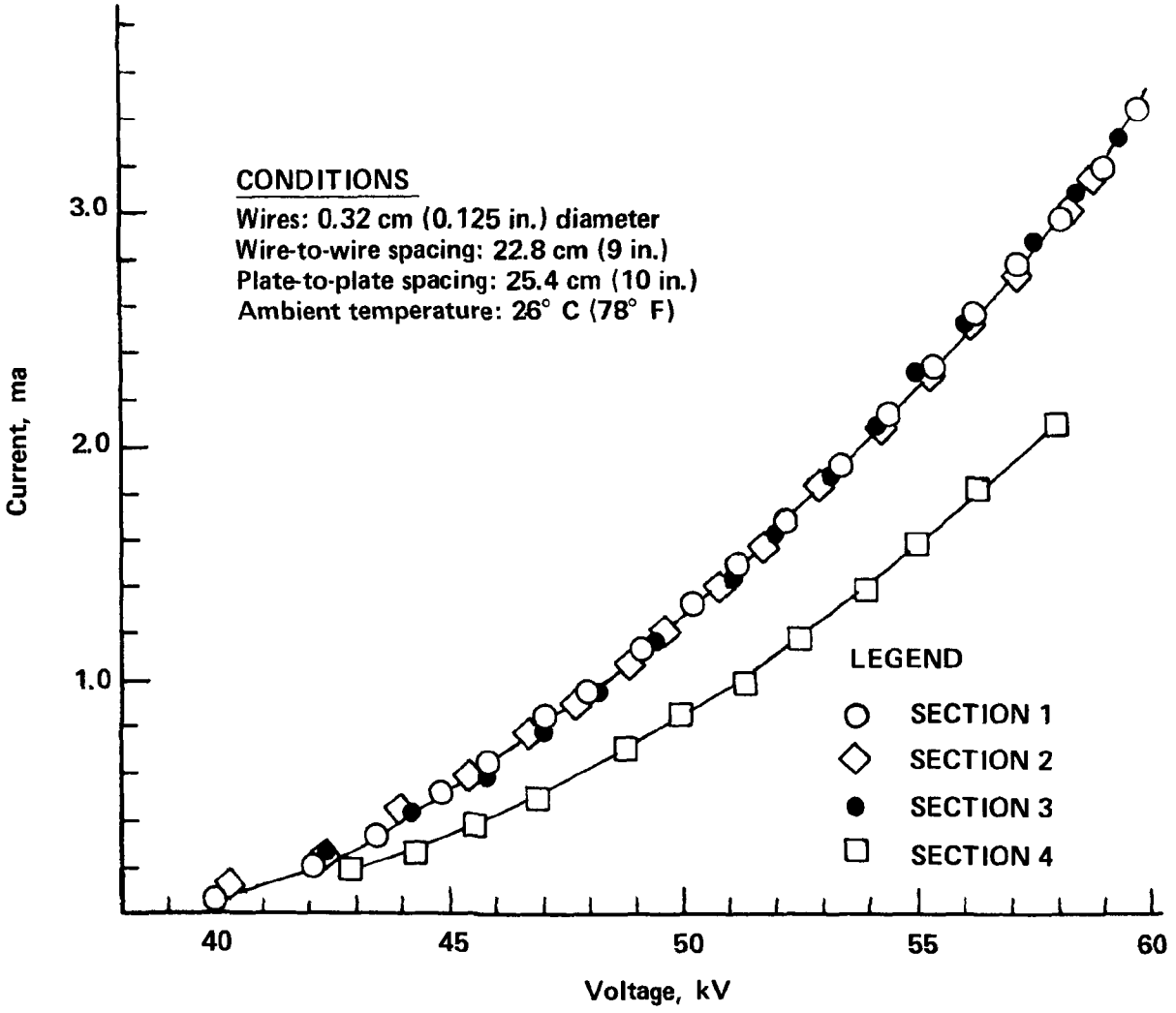

Figure 2.2 Clean-plate VI curve for pilot-scale ESP.

2.3 PARTICULATE MEASUREMENTS

Particulate Mass Concentrations

The particulate mass concentration in the pilot ESP is determined by collecting the particulate from a measured gas volume on a tared filter and determining the collected mass gravimetrically. The sample is collected isokinetically using a sharp-edged nozzle of 1.27-cm diameter stainless steel tubing. The sample is normally collected over 15 minutes, for a sample volume of 85-142 ℓ (3-5 ft^3). The sample is collected on a 49-mm glass fiber filter. The filter is placed in a labeled, disposable aluminum pan; filter and pan are weighed; the filter is inserted into the filter holder; and the sample probe assembled. The probe is then inserted in the duct, the sampling pump is started, and the flow rate is adjusted to give isokinetic sampling conditions. The sample is taken from the duct centerline.

After the sample has been collected, the filter is removed, placed in the same aluminum sample pan, and reweighed. Dust which collected in the filter holder is brushed into the pan. The nozzle and probe assembly are washed with acetone; the rinsings are collected in a second tared pan. The probe wash solvent is evaporated and the particulate mass remaining in the pan determined.

The total sampled mass is the sum of the filter and probe catches. The gas volume is measured with a dry gas meter. Approximate temperature corrections are made in the gas volume.

Particulate Size Distributions - Impactors

The primary particle sizing instrument used on the pilot ESP is the MRI* cascade impactor. The procedures used are generally those suggested by the manufacturer. The MRI impactor uses lightweight, removable collection substrates. For use on the pilot ESP, the substrates are coated with grease (Apiezon® L or H dissolved in toluene, the toluene then baked out).

---

*Meteorology Research, Inc., Box 637, Altadena, California 91001.

The impactor sample train consists of the sample nozzle, the impactor, temperature and pressure measurements after the impactor, an orifice for flow measurement, a dry gas meter, and the sample pump.

The orifice is used to set the sample flow rate, but gas meter readings are used for final data reduction. The measured gas rate through the impactor is corrected from meter temperature to stack temperature. The impactor substrates (in aluminum sample pans) are tared on a balance to a precision of 0.1 mg. Stage weights are determined after the sample run on the same balance.

Impactor data reduction requires that stage cut diameters (d_{50}'s) be determined for each stage from flow conditions and impactor parameters. The pilot ESP data are reduced using software developed for the TI-59 programmable calculator[1]. The data reduction utilizes the conventional impactor equation cast in the form:

$$d_{A50i} = \sqrt{\frac{0.135\ \mu\pi\ D_i^3 N_i K_{50i}}{Q \times 10^{-8}}} \qquad (1)$$

where: μ = viscosity of gas, poise
D_i = diameter of holes on ith stage, cm
N_i = number of holes on ith stage
Q = gas rate, ℓ/min
K_{50i} = impaction parameter for 50% collection efficiency on i^{th} stage
d_{A50i} = aerodynamic diameter at 50% collection efficiency on i^{th} stage.

The aerodynamic diameter (d_{A50i}) defined by this equation is that of Mercer and Stafford[2] and does not require calculation of the Cunningham slip correction factor.

For use, Equation 1 is rewritten in the form:

$$d_{A50i} = \sqrt{C_i \mu / Q \times 10^{-8}} \qquad (2)$$

where: C_i = stage constant for the ith stage, $C_i = 0.135\ \pi\ D_i^3 N_i K_{50i}$.

The constant C_i has been determined empirically for each stage of the MRI impactor.

The program receives as input the temperature, pressure, flow rate, and stage weights for the run. The output is in the form of stage d_{A50i}'s and the cumulative mass fraction of particulate smaller than the indicated d_{A50i}.

Particle penetrations as a function of size are also calculated using TI-59 software. The derivative of the function describing the cumulative undersize fraction (with respect to particle size) must be known for both inlet and outlet in order to calculate the penetration. A mathematical spline fit is used to achieve a smooth curve through the data generated in the impactor data reduction. The spline fit program fits the data, calculates derivatives at the desired particle diameters, and then calculates particle penetrations at those diameters.

Optical Particle Sizing

A Climet® Model 208 Particle Analyzer is used for optical particle sizing. The gas stream must be diluted to allow use of the Climet on the ESP inlet. The Climet provides directly the cumulative number of particles of sizes greater than 0.3 μm, 0.5 μm, 1.0 μm, 3 μm, 5 μm, and 10 μm diameters (as calibrated with polystyrene latex spheres). Data is reduced to particles of a given size by assigning the incremental number of particles between two diameters to the geometric mean of the two diameters. For example, if 1.3×10^6 particles are counted as greater than 0.3 μm in size, and 0.7×10^6 particles counted as greater than 0.5 μm, the difference, 600,000, is the number of particles between 0.3 and 0.5 μm. If it is necessary to assign a size to this data to plot a distribution, the geometric mean of the sizes is used.

Velocity Measurements

Gas velocities in the ESP are calculated from the orifice plate measurements made at the flow controller.

Light Absorption Measurements

The MRI Plant Process Visometer (PPV) is used to measure light absorption within the ESP. The PPV indicates real time trends in the particle concentrations.

3.0 PRELIMINARY PRECHARGER EXPERIMENTS, MARCH 1978

3.1 INTRODUCTION

The presence of high resistivity dust (>$5x10^{10}$ Ω•cm) reduces the efficiency of an ESP. This is thought to be due to a reduction in particle charging effectiveness. The high resistivity dust experiences high internal electric fields and subsequent electrical breakdown and back-corona. The back-corona produces a bipolar ion field; competing effects of the negative and positive ions result in reduced net charging efficiency.

In research sponsored by EPA, Southern Research Institute has devised and investigated the performance of a three-electrode system for controlling the effects of back-corona. The device, a particle precharger, includes both of the usual electrodes, the discharge "wire" and the passive "plates." In addition, it includes a screen electrode, biased to a high negative voltage relative to the plate, but lower than the wire voltage. The screen is placed close to the plate (≈ 2 cm). Negative ions generated close to the wire and the particles to which they attach are able to proceed from wire to plate without much interference from the screen (the negative screen bias repels the negative ions). The particles are collected on the plate as desired. However, the positive ions generated by the onset of back-corona are attracted to the screen and captured, improving the net charging effect.

Following the precharger in an operating ESP is a collector section (for this experiment the remainder of the pilot-scale ESP served as the collector). If the precharger works well, the particle leaving the precharger is adequately charged; corona in the collector section is then unnecessary. For maximum efficiency the collector section should be operated with a minimum of current and high electric fields. Thus collector design should be somewhat different from normal ESP design, attempting to minimize corona while maintaining the electric field.

Laboratory tests were encouraging[3] and, in an effort to prove out the concept on a larger scale, a precharger was designed and built for use on the IERL-RTP pilot ESP.

The precharger replaced the transition section of the ESP for testing. Figure 3.1 shows the approximate dimensions and configuration of the pilot precharger.

3.2 DESIGN OF EXPERIMENT

Operation of the pilot precharger was tested at the IERL-RTP ESP on March 15, 16, and 21, 1978, in three runs. Operating conditions for the ESP are:

Gas Flow:	22.7 m^3/min (800 cfm) on March 15 and 16, 1978 28.3 m^3/min (1000 cfm) on March 21, 1978
Temperature:	149°C (300°F)
Plate Spacing:	25.4 cm (10 in.)
Wires:	11 wires per section, 10.2 cm (4 in.)
Dust :	flyash injected by sandblast guns
Rapping:	manual; frequency not recorded
Electrical:	attempted to maintain 0.1 to 0.2 mA current in each section at a voltage just below the spark level.
	March 15, 1978: 0.1 to 0.2 mA current at 41 to 48 kV at start, 36-42 kV at end
	March 16, 1978: 0.1 to 0.2 mA current, voltage not recorded
	March 21, 1978: current erratic, 0.64 to 1.47 mA at start, 1.1 to 3.07 mA at end.

The testing included total particulate mass sampling at inlet and outlet, impactor particle size determinations at inlet and outlet, and monitoring of precharger operation.

The precharger was off during the March 15 run, and on during the March 16 and March 21 runs. When in operation, the discharge wire current and the screen voltages were both kept constant; corona wire voltage was nearly constant throughout the tests. An abbreviated data sheet for the runs is presented in Table 3.1.

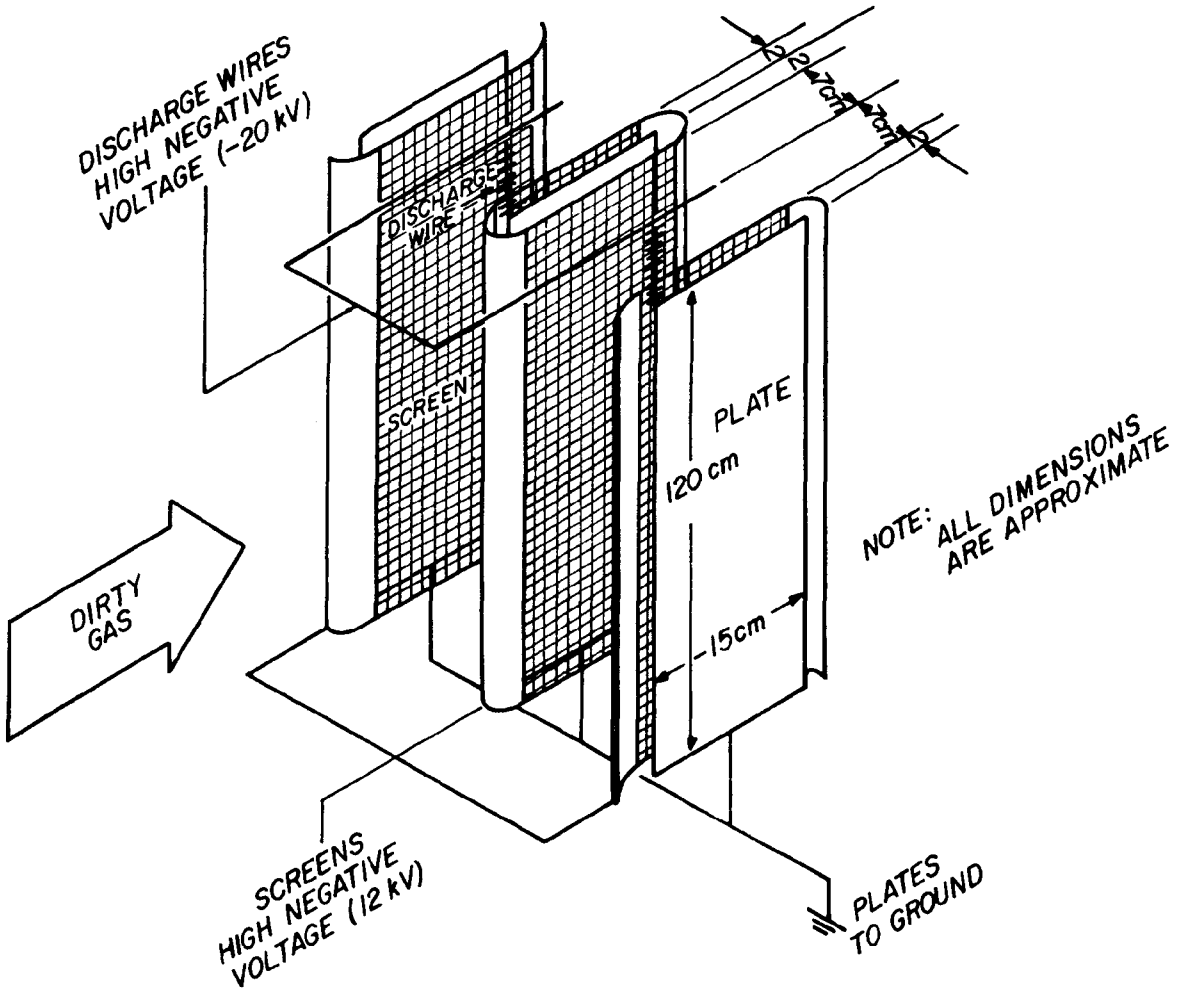

Figure 3.1 Schematic drawing of EPA/SoRI precharger, March 1978.

Table 3.1. Precharger Runs, March 1978

	Date (1978)		
	3/15	3/16	3/21
Dust Loading, g/m^3			
Inlet	0.405	0.422	0.307
Outlet	0.164	0.058	0.078
ESP Efficiency, %	59.6	86.2	74.4
MMD, μm			
Inlet	6.97	7.28	6.04
Outlet	4.58	3.72	4.99
Precharger	Off	On	On
Flow, m^3/min	22.6	22.6	28.3
Temp., °C	149	149	149

3.3 RESULTS

Inlet and outlet size distributions for the three runs are presented in Figure 3.2. Penetrations as a function of particle size are presented in Figure 3.3. Precharger operating parameters throughout the March 16 and 21 runs are presented graphically in Figures 3.4 and 3.5, respectively.

ESP efficiency was somewhat higher during the precharger operation, although this was not an exhaustive test. Problems with the ESP current during the March 21 run make that data difficult to evaluate. The tests served best to prove out several features of precharger operation and allow better design of a second generation unit which has since been installed at the IERL-RTP pilot ESP. Collector design to prevent problems such as the instability which occurred on March 21 has been one of the major points investigated.

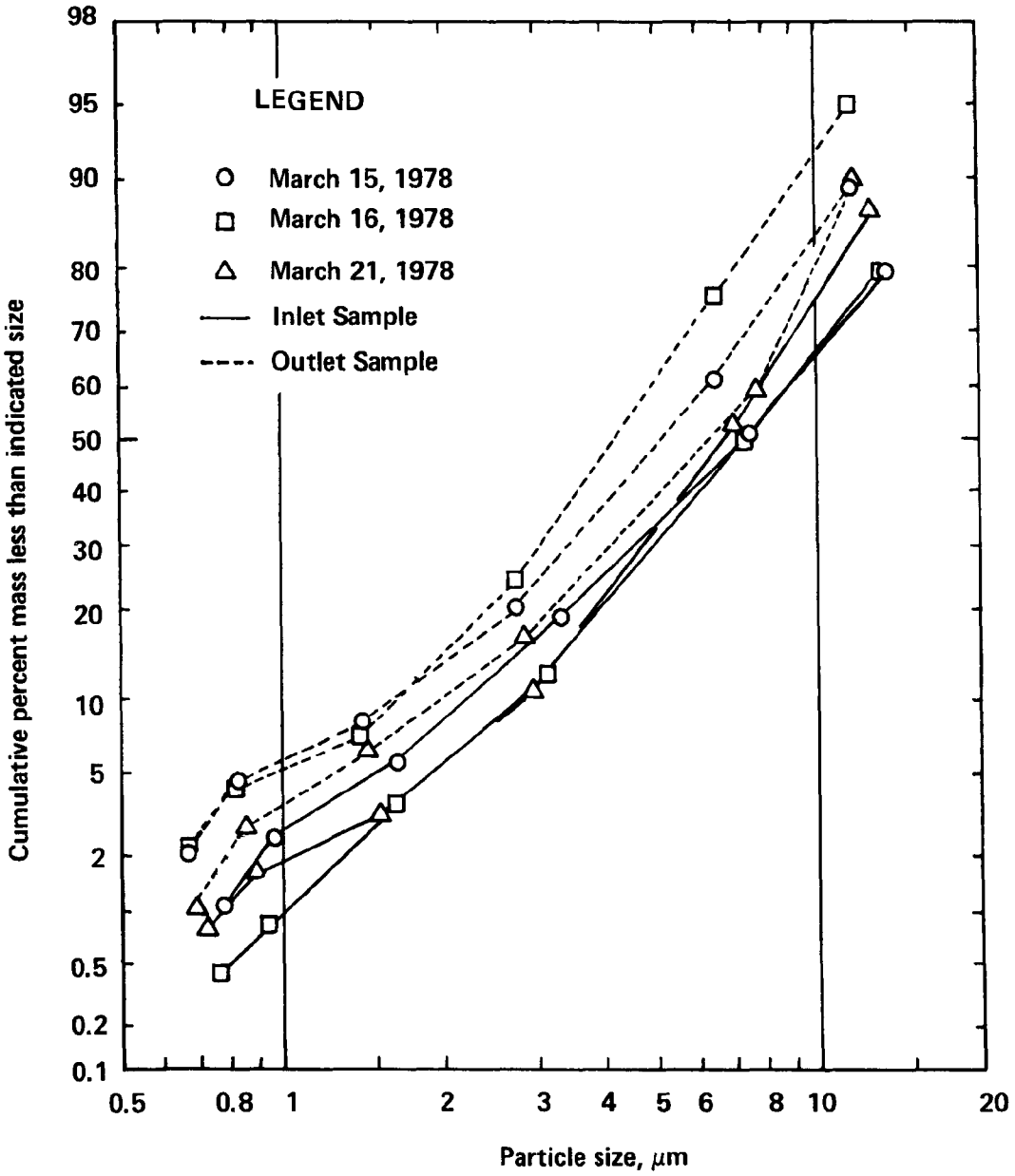

Figure 3.2 Inlet and outlet size distributions, precharger runs.

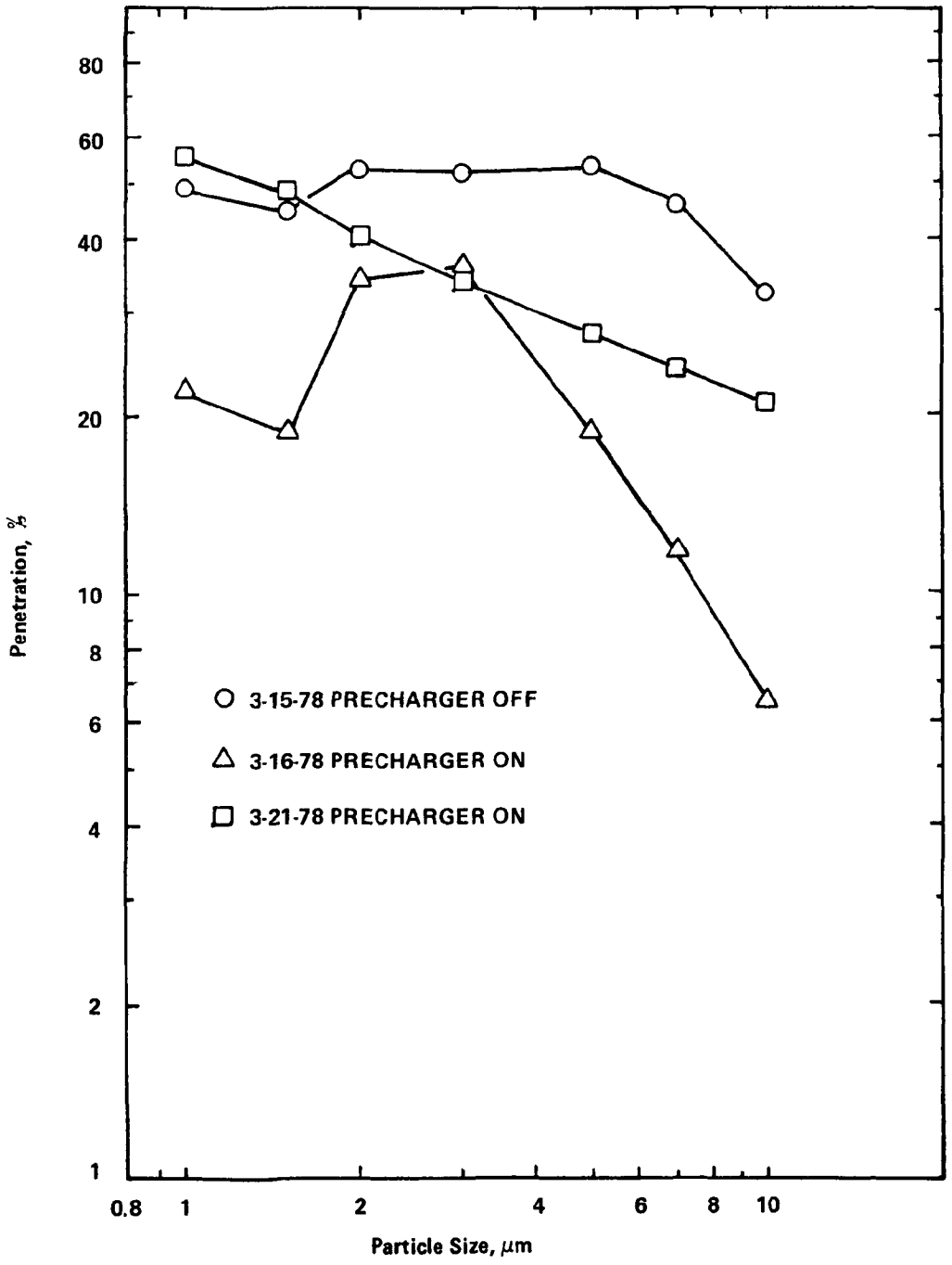

Figure 3.3 Penetrations for precharger runs.

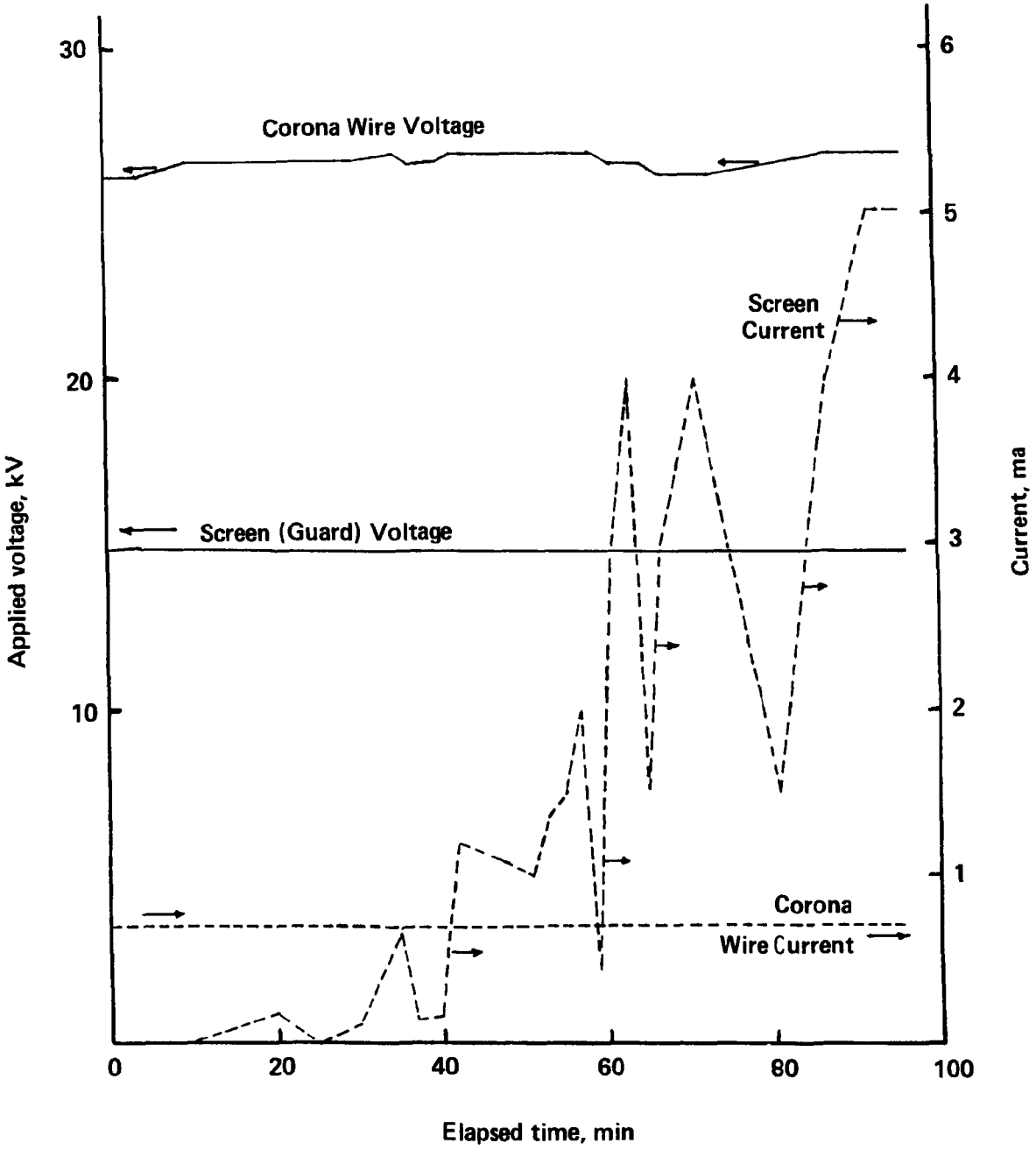

Figure 3.4 Precharger operating parameters, March 16, 1978.

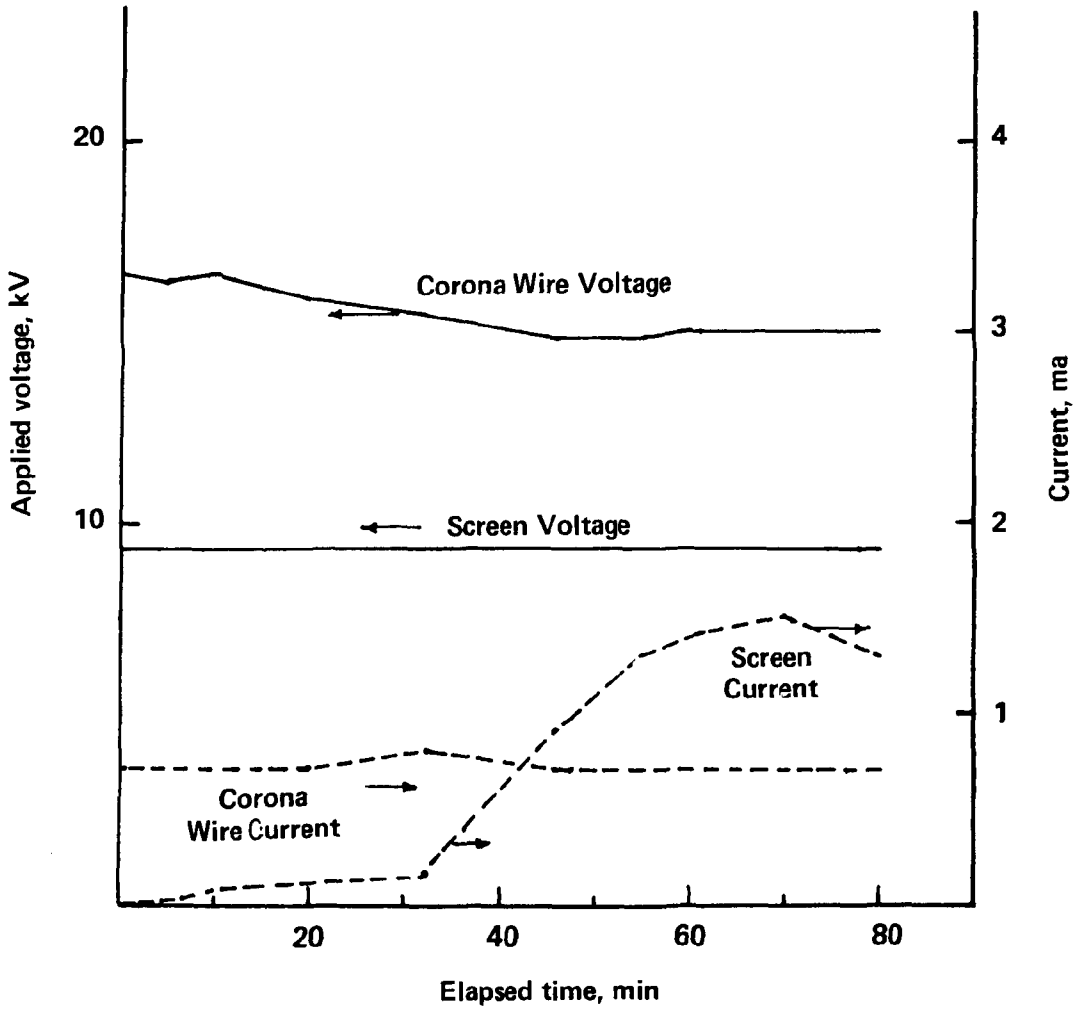

Figure 3.5 Precharger operating parameters, March 21, 1978.

4.0 ESP EFFICIENCY RUNS

4.1 INTRODUCTION

The general operating characteristics of the pilot ESP, with particular attention to efficiency, were investigated with two sets of runs: one set of three runs was initiated in late March 1978; the other comprised 9 days of operation in mid-May 1978. The run conditions for these 12 runs are summarized in Table 4.1, along with particulate mass loadings, mean diameters, and overall efficiency values.

4.2 RESULTS

Figure 4.1 is a presentation of overall efficiency as a function of inlet mass median diameter (MMD). The runs made in March differ noticeably from those runs made in May. The obvious differences are in gas rate (higher in May) and temperature (lower in May). For the March runs, inlet MMD made little difference with respect to efficiency; back-corona problems required that the voltage be reduced from the March 28 run to the March 29 run, then even further to the March 30 run. The reduction in field strength dominates, leading to reduced efficiency. For the May runs, inlet MMD was a stronger variable. We must assume that these runs were fairly constant electrically, although the electrical data were not recorded.

Particle penetration as a function of size is presented in Figures 4.2 and 4.3 for the March and May runs.

Table 4.1. ESP Conditions During Efficiency Runs

Date (1978)	MMD, μm Inlet	MMD, μm Outlet	Mass Loading, mg/m³ Inlet	Mass Loading, mg/m³ Outlet	Efficiency, %	Temperature, °C	Gas Rate, m³/min	Comments
3/28	10.2	5.64	0.453	0.0280	93.8	149	22.6	Voltage 38 to 42 kV at start; 25 to 35 kV at end Current 0.45 to 1.1 mA at start; 1.5 to 3.4 mA at end
3/29	9.62	6.79	0.416	0.0624	85.0	149	22.6	Voltage 28 to 35 kV at start; 24 to 32 kV at end Current 1.1 to 1.8 mA at start; 1.6 to 5.6 mA at end
3/30	10.0	7.3	0.391	0.0984	74.8	149	22.6	Voltage 28 to 31 kV at start; 24 to 27 kV at end Had problems with back-corona.
5/8	8.51	3.57	0.132	0.0126	90.5	16	34.0	
5/10	9.33	3.15	0.327	0.0203	93.8	19	34.0	
5/11	10.1	2.45	0.459	0.0053	98.8	17	34.0	
5/12	13.8	2.1	1.820	0.0074	99.6	17	34.0	
5/15	9.09	2.43	0.148	0.0153	89.7	13	34.0	
5/16	9.56	3.18	0.810	0.0227	97.6	16	34.0	
5/17	6.10	1.97	0.797	0.0152	98.1	17	34.0	
5/18	14.3	1.73	1.014	0.0035	99.65	19	34.0	
5/20	9.46	3.67	1.18	0.0359	96.77	20	34.0	

NOTES: Plate spacing: 25.4 cm. Wires: 7 wires/section at 17.8 cm spacing. Electrical: Maximum voltage without causing sparking. Rapping: manual.

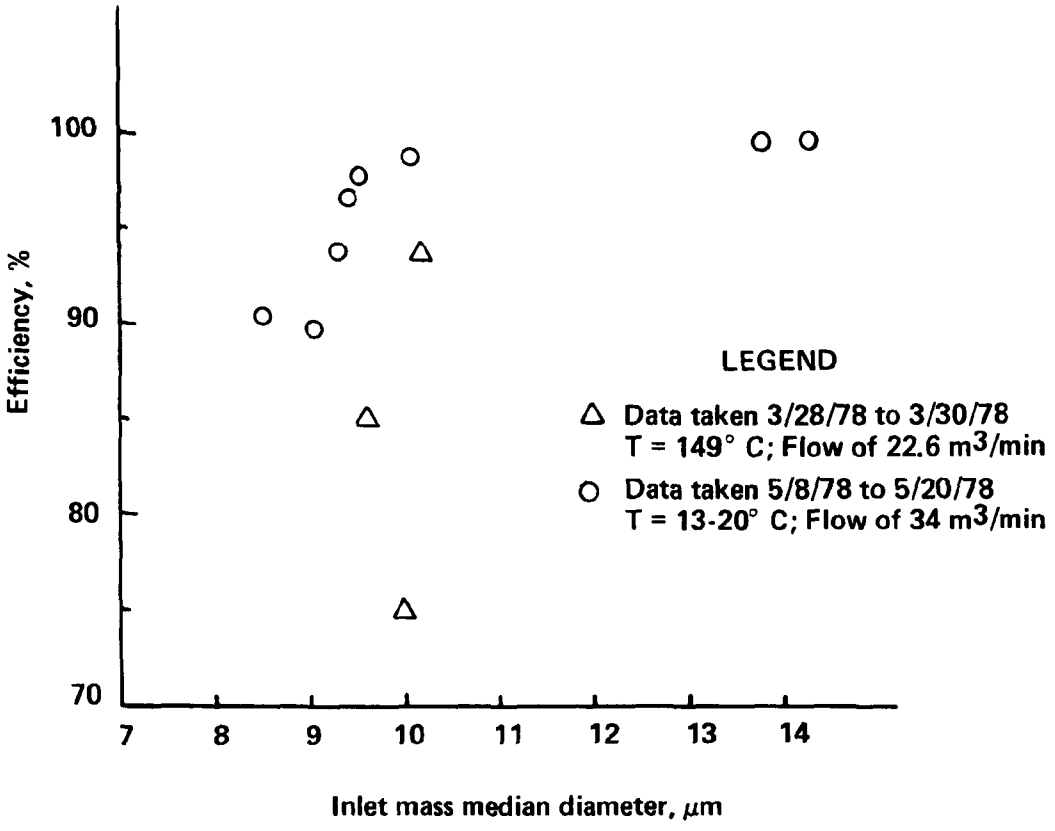

Figure 4.1 Effect of inlet particle size on efficiency.

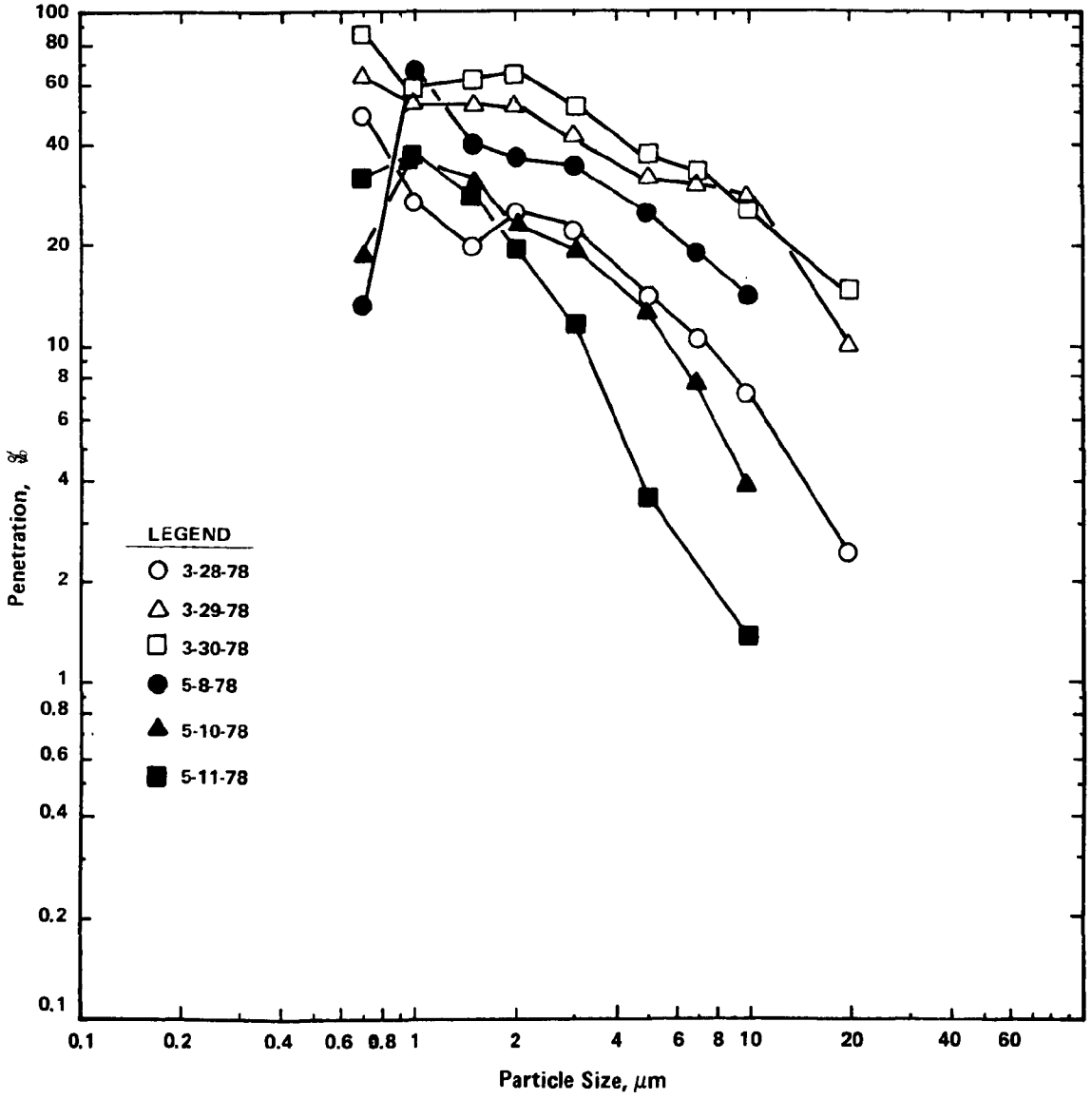

Figure 4.2 Particle penetrations; efficiency runs 3/28/78 to 3/30/78 and 5/8/78 to 5/11/78.

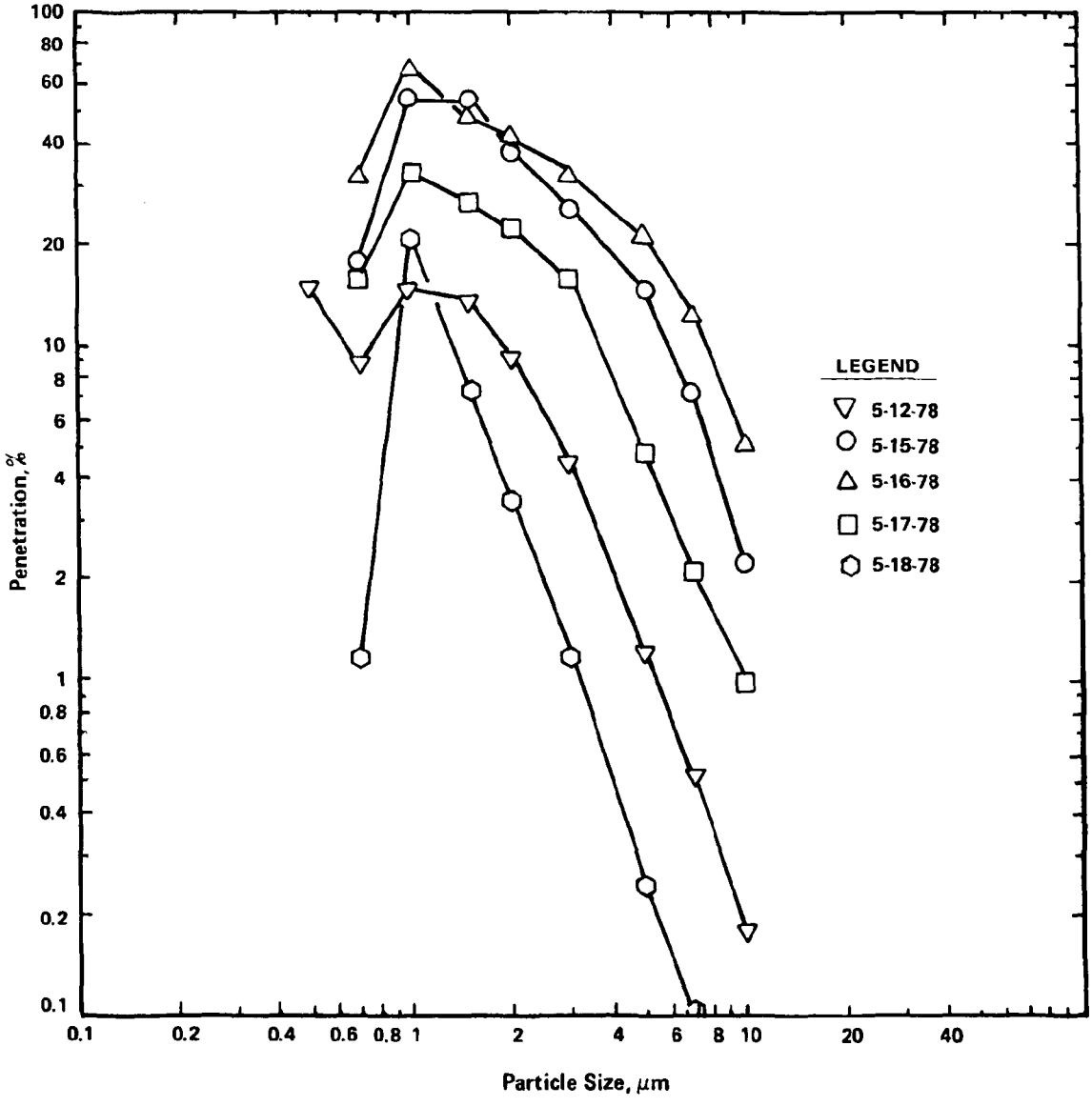

Figure 4.3 Particle penetrations, efficiency runs, 5/12/78 to 5/17/78.

5.0 REENTRAINMENT STUDIES

5.1 INTRODUCTION

An investigation of ESP reentrainment was initiated in early April 1978. The test work was designed to look primarily at the effects of sparking within the ESP. The ESP was loaded with dust by operating with both flyash injection and ESP on. The flyash feed was stopped once the ESP was loaded, and particle distributions at the outlet were monitored using the Climet particle counter. Various sections of the ESP were turned on and off, and sections were made to spark with the downstream sections on and off. Table 5.1 summarizes the operating conditions for both test days and presents the particle number distributions.

5.2 RESULTS

Total particle counts for the two days of operation are presented in Figures 5.1 and 5.2. Looking first at the April 8 data, Figure 5.1, it can be seen that the effects of sparking are noticeable in the particle counts. Sparking in sections 1, 3, and 4 produced higher particle counts than were present without sparking, even though downstream precipitator sections were on. Sparking in section 2 did not produce high counts. The April 7 data (Figure 5.2) are not completely consistent with those taken April 8. Sparking produced high particle counts only when sections 1 and 3 were sparked. For sections 1 and 2, data were collected under sparking conditions with the downstream sections on and off. In both cases, having the collector sections on reduced the particle count.

The "outlet, power on" versus the "outlet, power off" data collected April 7 indicates that particles reentrained by viscous forces could be significant; the April 8 data contradicts this position, indicating that sparking is the major contributor to reentrainment.

Figures 5.3, 5.4, and 5.5 present the particulate distributions for the reentrainment study. The distributions are cumulative number percent with size greater than indicated. As represented, larger distributions are above and to the left of the smaller distributions. The size distribution

Table 5.1. Sumary of the Operating Conditions and the Number Distributions (April 7 and 8, 1978)

Run Description	Number of Percent with Size > Indicated Size					
	0.3 μm	0.5 μm	1.0 μm	3.0 μm	5.0 μm	10.0 μm
4/7/78						
Inlet	100.0	6.24	0.32	0.01	0.00	0.00
Outlet (Power on, 0.2 mA)	100.0	4.39	0.21	0.00	0.00	0.00
Outlet (Power off)	100.0	6.45	0.44	0.02	0.00	0.00
Spark 1; Power on 2,3,& 4	100.0	29.15	5.67	0.04	0.01	0.00
Spark 1, Power off	100.0	25.01	6.30	0.17	0.06	0.01
Spark 2, Power off 3 & 4	100.0	15.04	2.98	0.03	0.01	0.00
Spark 2, Power on 1,3 & 4	100.0	19.83	3.48	0.03	0.01	0.00
Spark 3, Power on 1,2 & 4	100.0	40.99	12.18	0.36	0.10	0.02
Spark 4, Power on 1,2 & 4	100.0	25.10	5.28	0.04	0.01	0.00
4/8/78						
Inlet - Dust feed off	100.0	6.78	0.66	0.03	0.01	0.00
Outlet - Dust feed on, 0.20 mA power on	100.00	66.98	20.97	0.28	0.08	0.01
Outlet - Feed off, power on	100.00	12.65	1.66	0.06	0.01	0.00
Outlet - Spark 1; 2,3, & 4 on	100.00	37.74	14.18	1.03	0.29	0.04
Outlet - Spark 2; 1,3, & 4 on	100.00	21.88	5.03	0.28	0.10	0.01
Outlet - Spark 3; 1,2, & 4 on	100.00	40.91	14.10	1.23	0.37	0.06
Outlet - Spark 4; 1,2, & 3 on	100.00	52.04	21.68	2.02	0.07	0.10
Outlet - Power off	100.00	10.70	1.66	0.10	0.03	0.00
Power on Sec. 1; 2,3, & 4 off	100.00	8.53	1.04	0.03	0.02	0.00

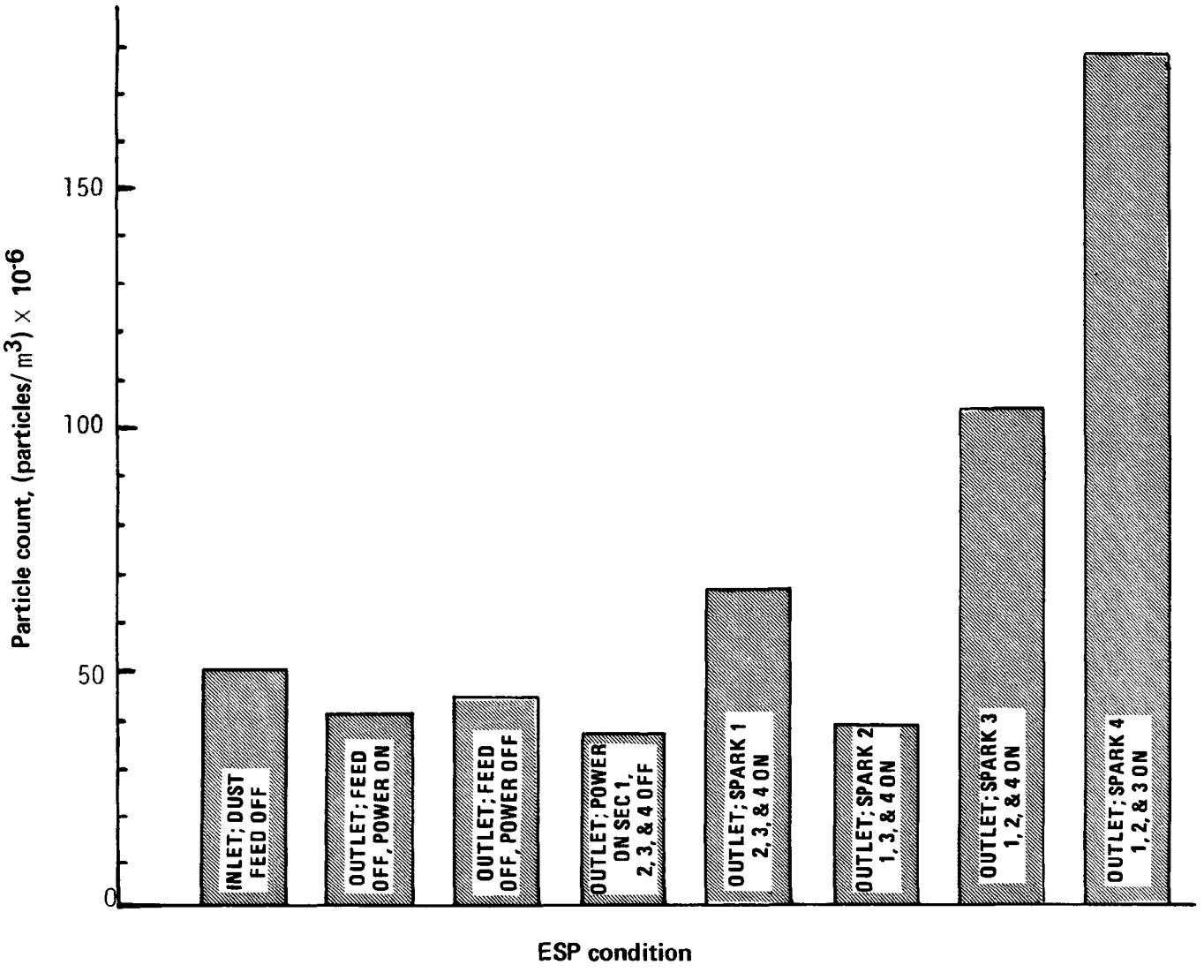

Figure 5.1 Reentrainment study, April 8, 1978

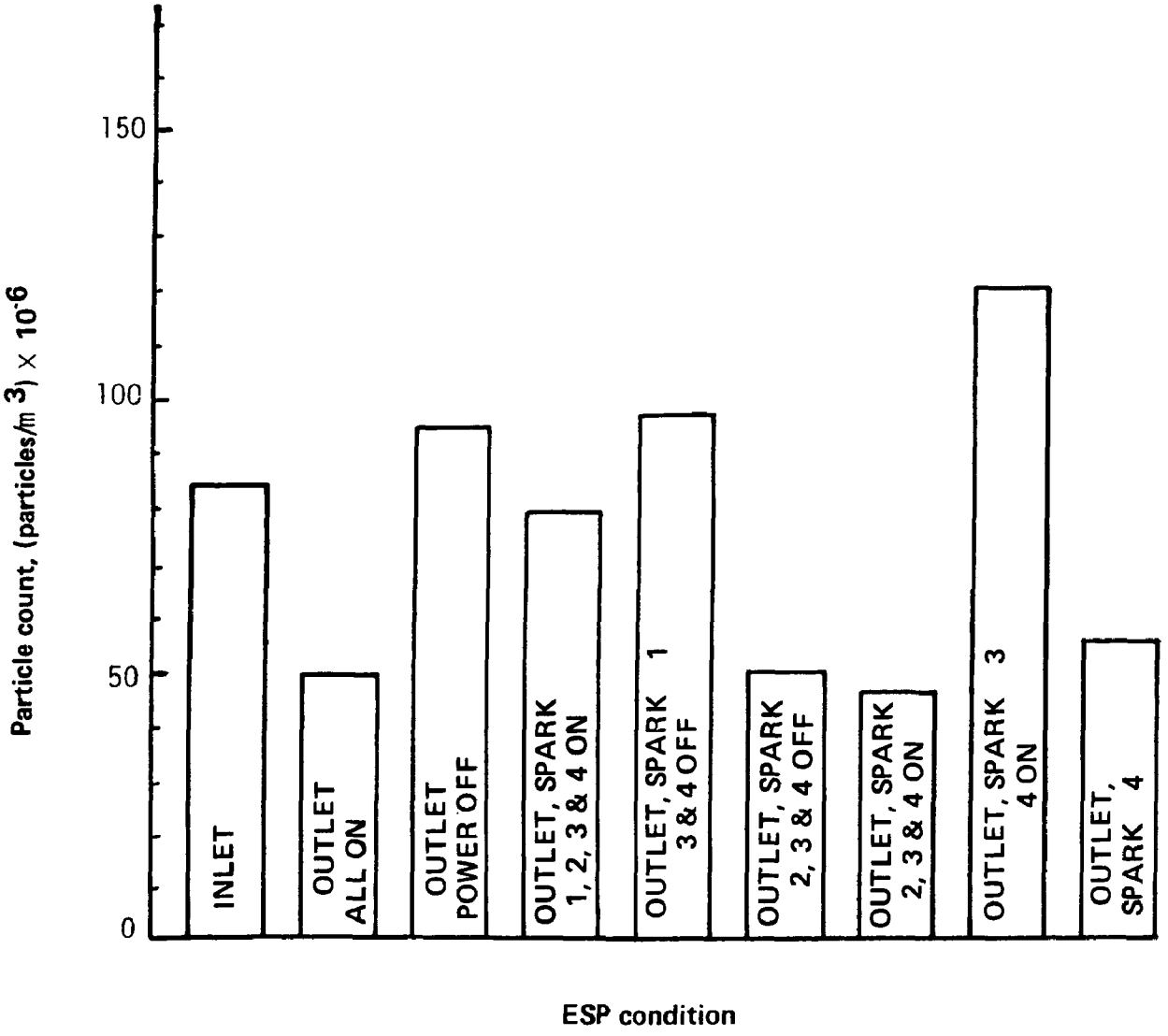

Figure 5.2 Reentrainment study, April 7, 1978.

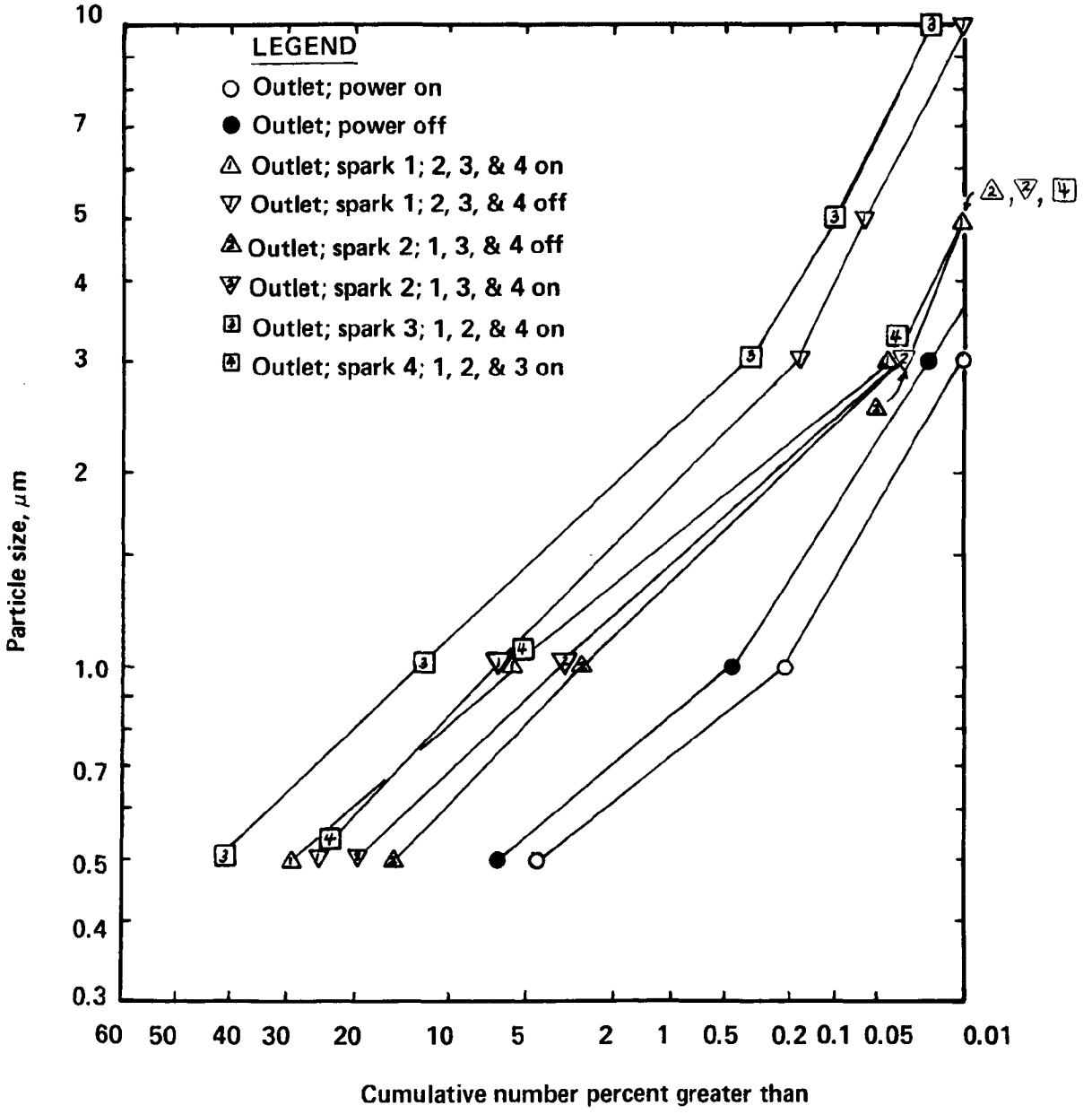

Figure 5.3 Size distributions for April 8, 1978, reentrainment study.

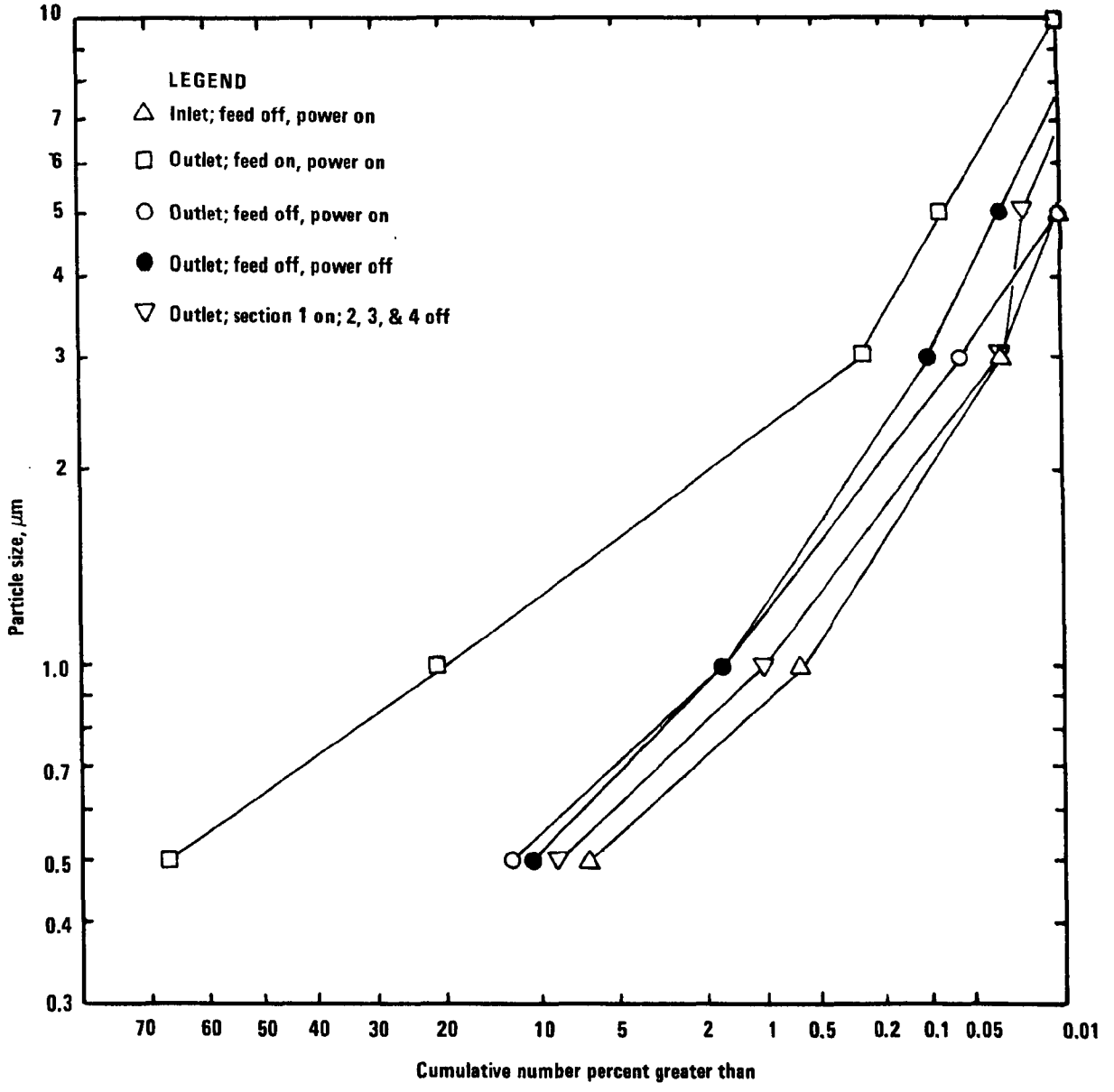

Figure 5.4 Size distributions for April 7, 1978, reentrainment study.

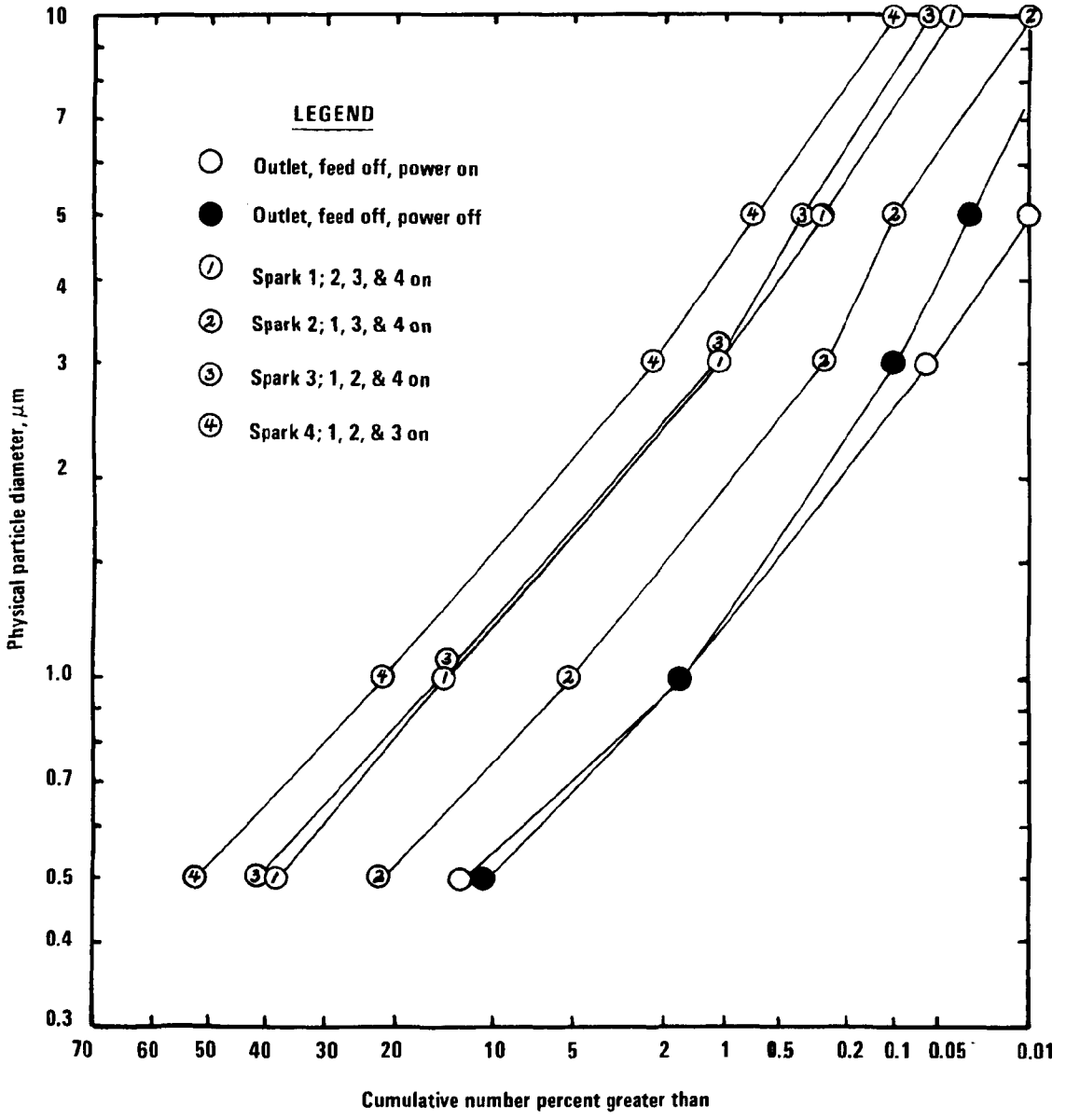

Figure 5.5 Size distributions for April 7, 1978.

data indicate that sparking produces larger particulate than that produced by other reentrainment mechanisms. This was true for both days' runs. No pattern of size distribution change was established with regard to the section sparked.

6.0 PARAMETER VARIATION WITH POSITION IN ESP

6.1 INTRODUCTION

A series of experimental runs was made in May and June 1978 to investigate the consistency of particle parameters within the ESP. The tests consisted of impactor and velocity traverses at the ESP inlet (with the ESP power off) as well as some data at other sample ports. The vertical particle size distribution was not examined in this series of runs.

6.2 DESIGN OF EXPERIMENT

The ESP was operated at 25.4 cm plate spacing throughout the particle size distribution runs (5-31-78 to 6-5-78). The temperature was ambient except for the June 7 run, when it was raised to about 80°C. Flyash injection was by sandblast gun. The flow rate was kept constant at about 107 m/min during the test.

6.3 RESULTS

Figure 6.1 presents the velocity distribution both horizontally and vertically at the inlet. Considerable variation between sampling ports is evident; across the duct the velocity profile appears relatively flat to within 2 cm or so of the ESP sidewall. The velocity distribution is less uniform at the bottom sample port, probably due to the baffles. These velocity distribution data are fairly consistant with those obtained previously, although the variation at the bottom of the duct is larger than expected. Figure 6.2 is another velocity distribution measured the following day. Figure 6.3 is a presentation of mass loading as a function of probe position. The loadings close to the wall are about 20 percent above the average for each day. The mass mean diameter data presented in Figure 6.4 show a general trend for an increase in particle size as the probe nears the wall. The incomplete data from June 6 contradict this trend near the center of the ESP.

The complete particle distributions for the runs presented in Figure 6.4 are presented in Figures 6.5, 6.6, and 6.7 (for May 31, June 1, and June 5, respectively). The complete distributions for May 31 and June 1

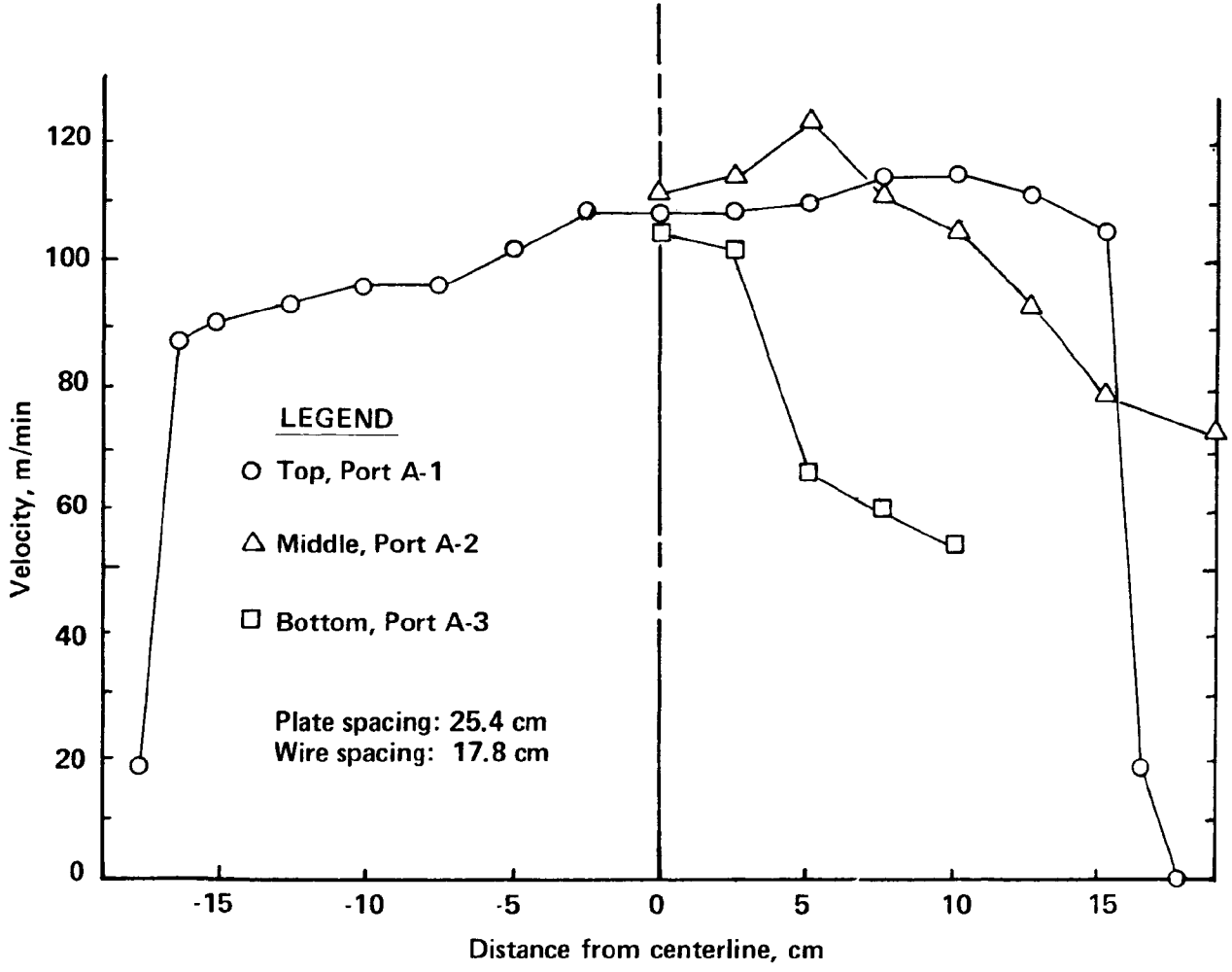

Figure 6.1 Velocity distribution in ESP, May 30, 1978.

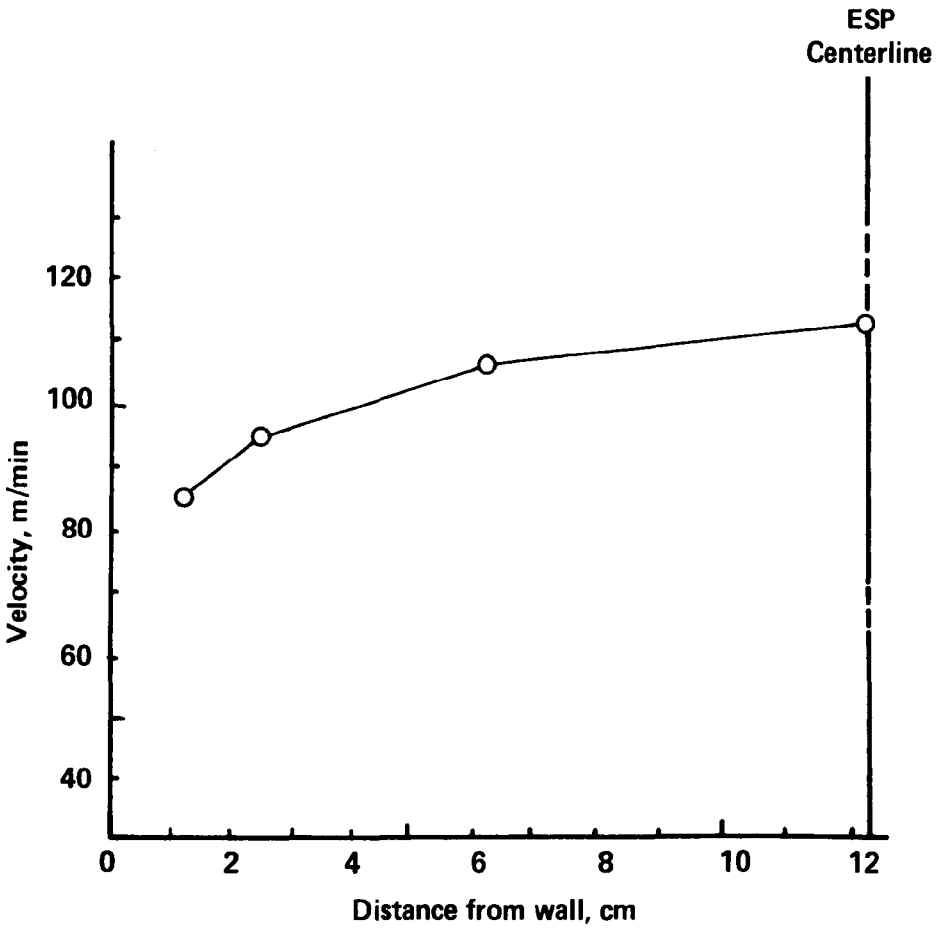

Figure 6.2 Velocity distribution in ESP, May 31, 1978.

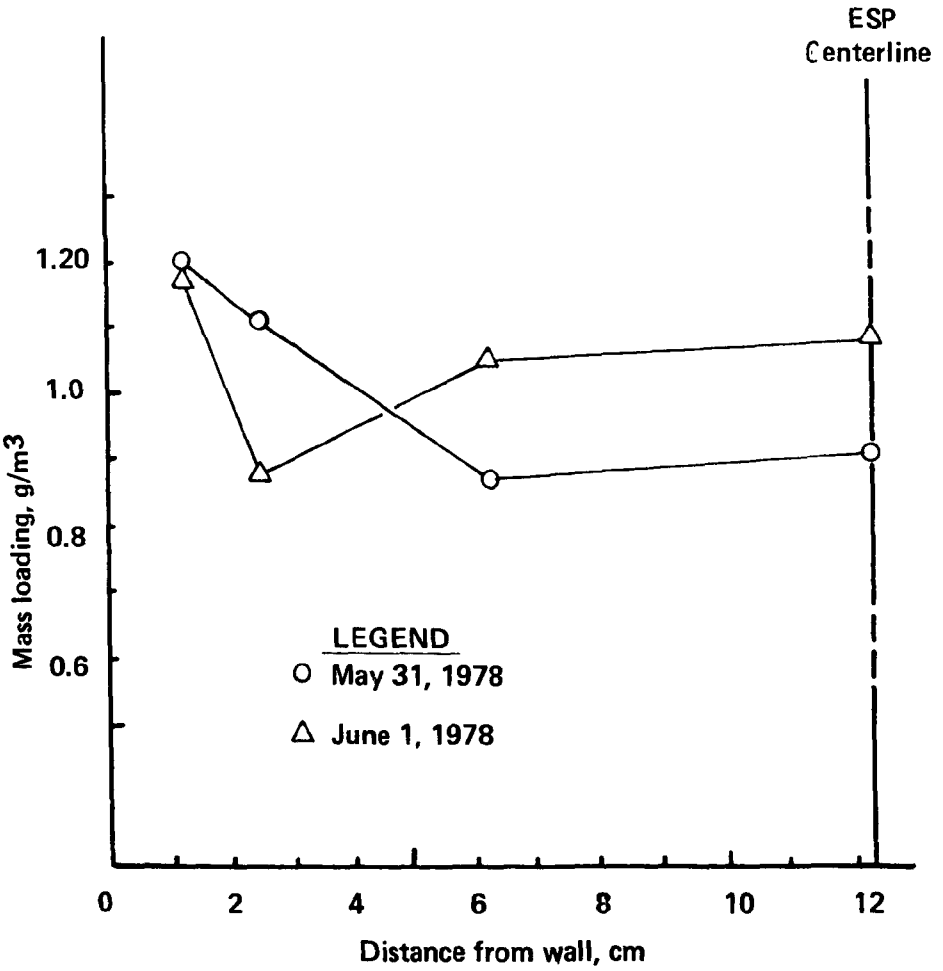

Figure 6.3 Mass loading variation in ESP.

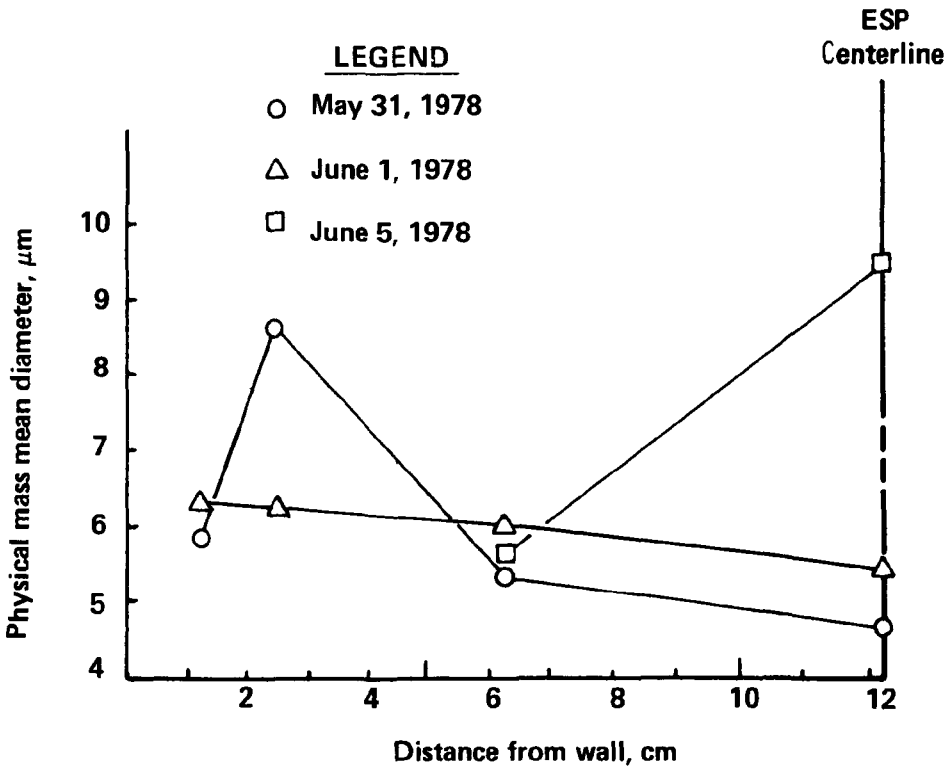

Figure 6.4 Variation of size distribution within ESP.

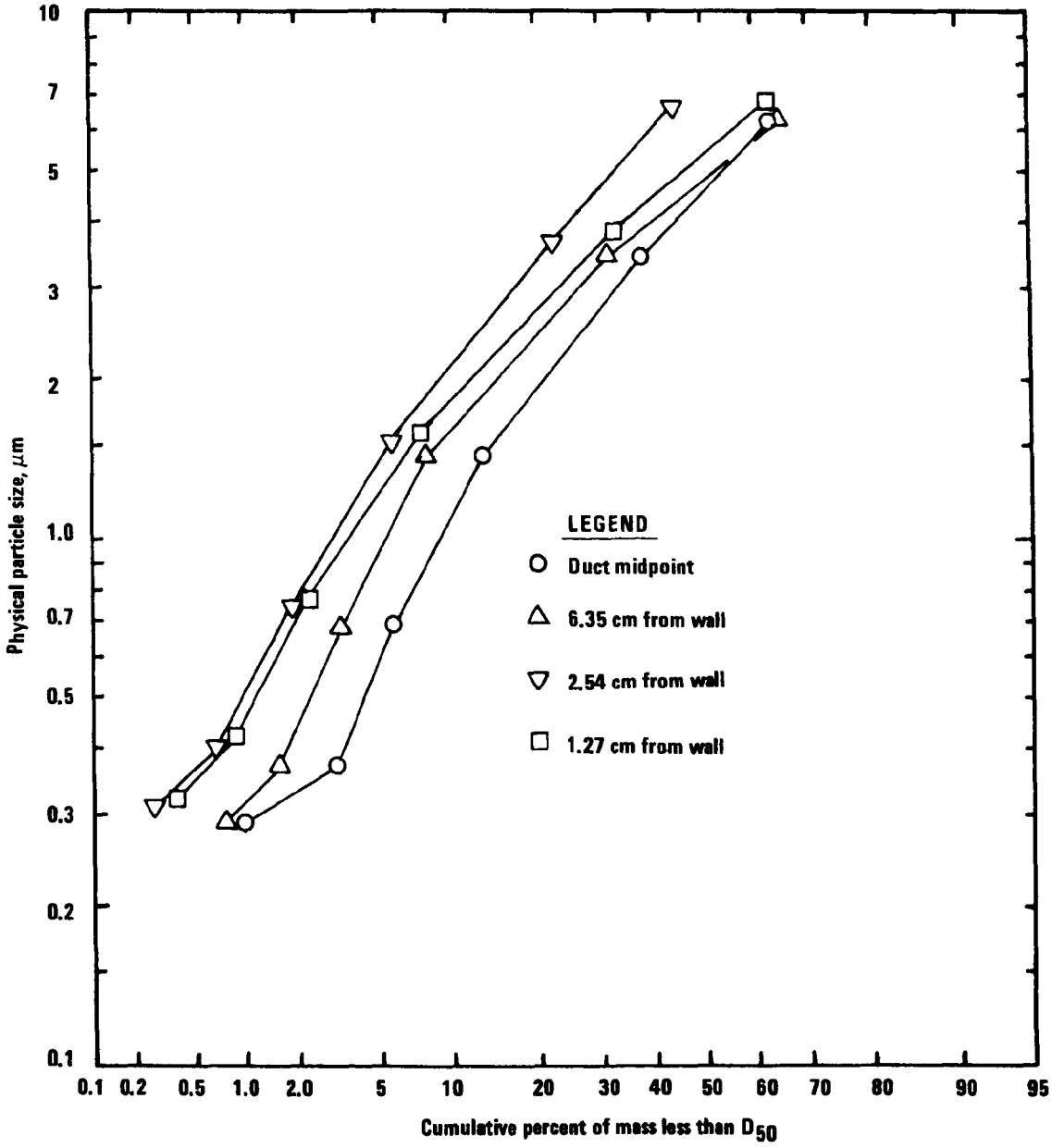

Figure 6.5. Particle size distributions at different sampling locations, May 31, 1978.

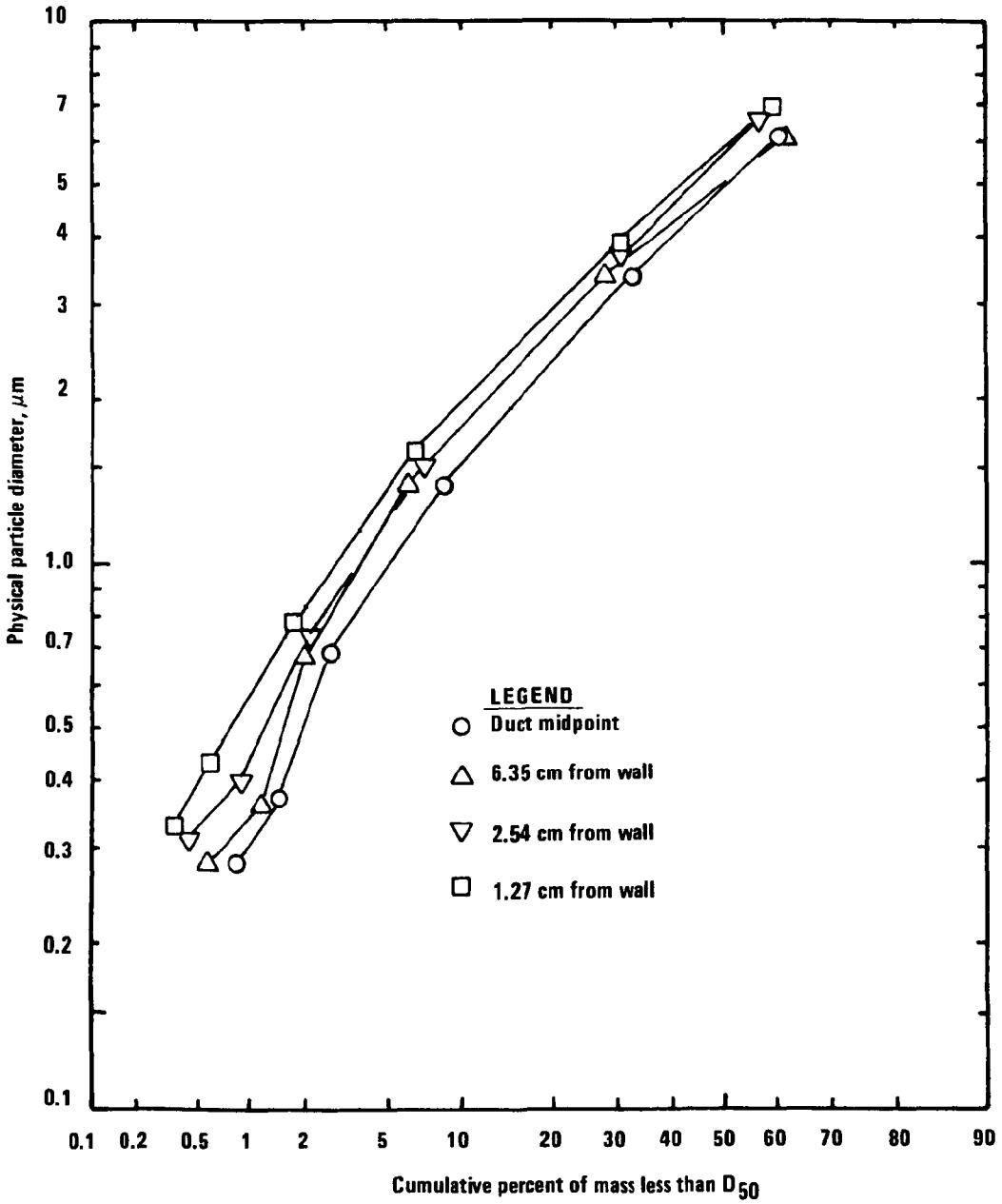

Figure 6.6 Particle distributions at different sampling points, June 1, 1978.

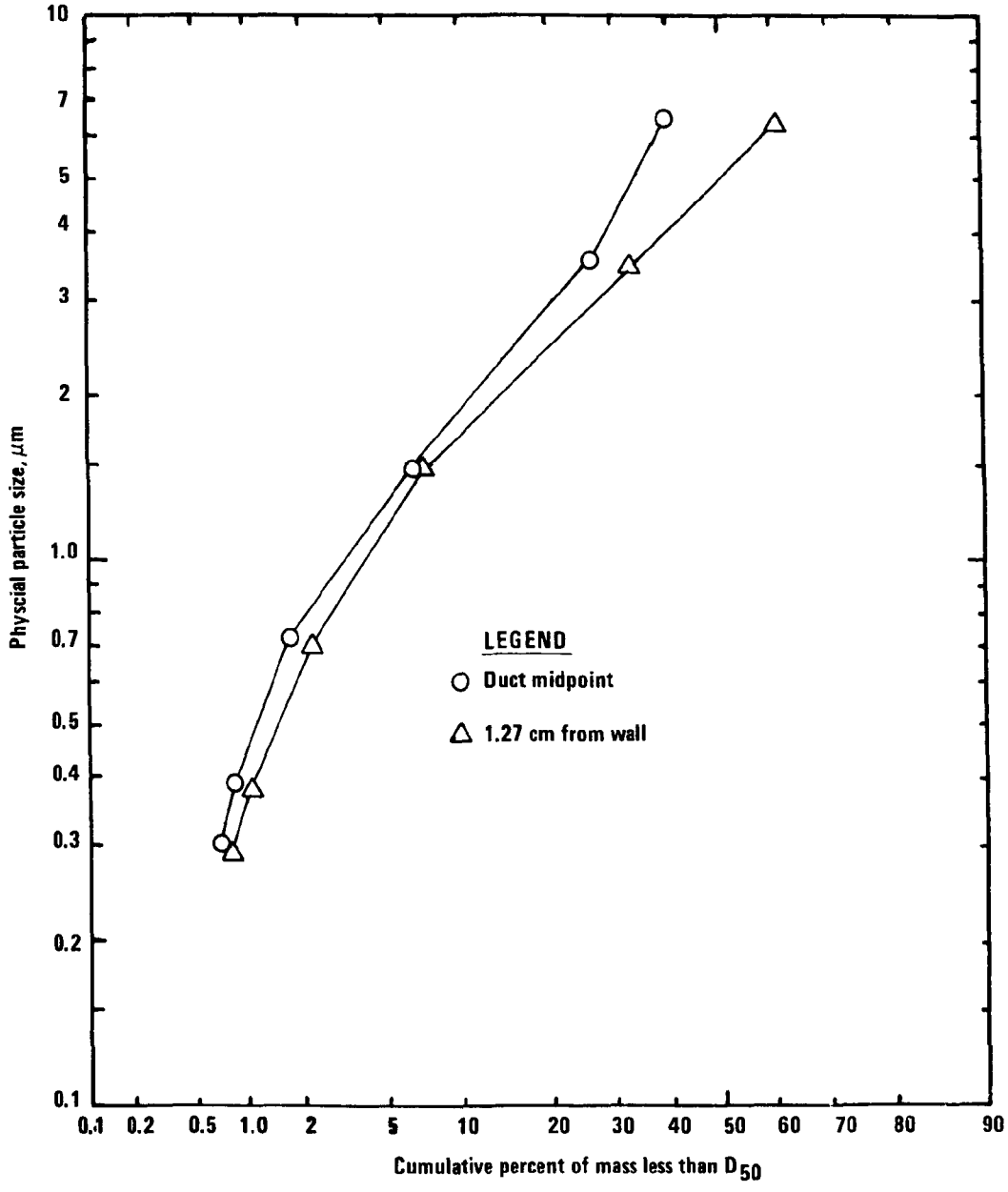

Figure 6.7 Particle size distributions at different sampling positions, June 5, 1978.

show a general particle size increase closer to the precipitator wall; the June 5 data, at two locations only, increase in size toward the duct center.

Figures 6.8 and 6.9 present data from five essentially replicate runs made over 2 days. Two of the runs, 6-6-1 and 6-7-1, involved operation of the dust feed equipment without auxiliary heat; the other three runs included some form of heat, as indicated. The trend is for larger particle size distributions with the heated dust injection equipment, although it is not a strong trend.

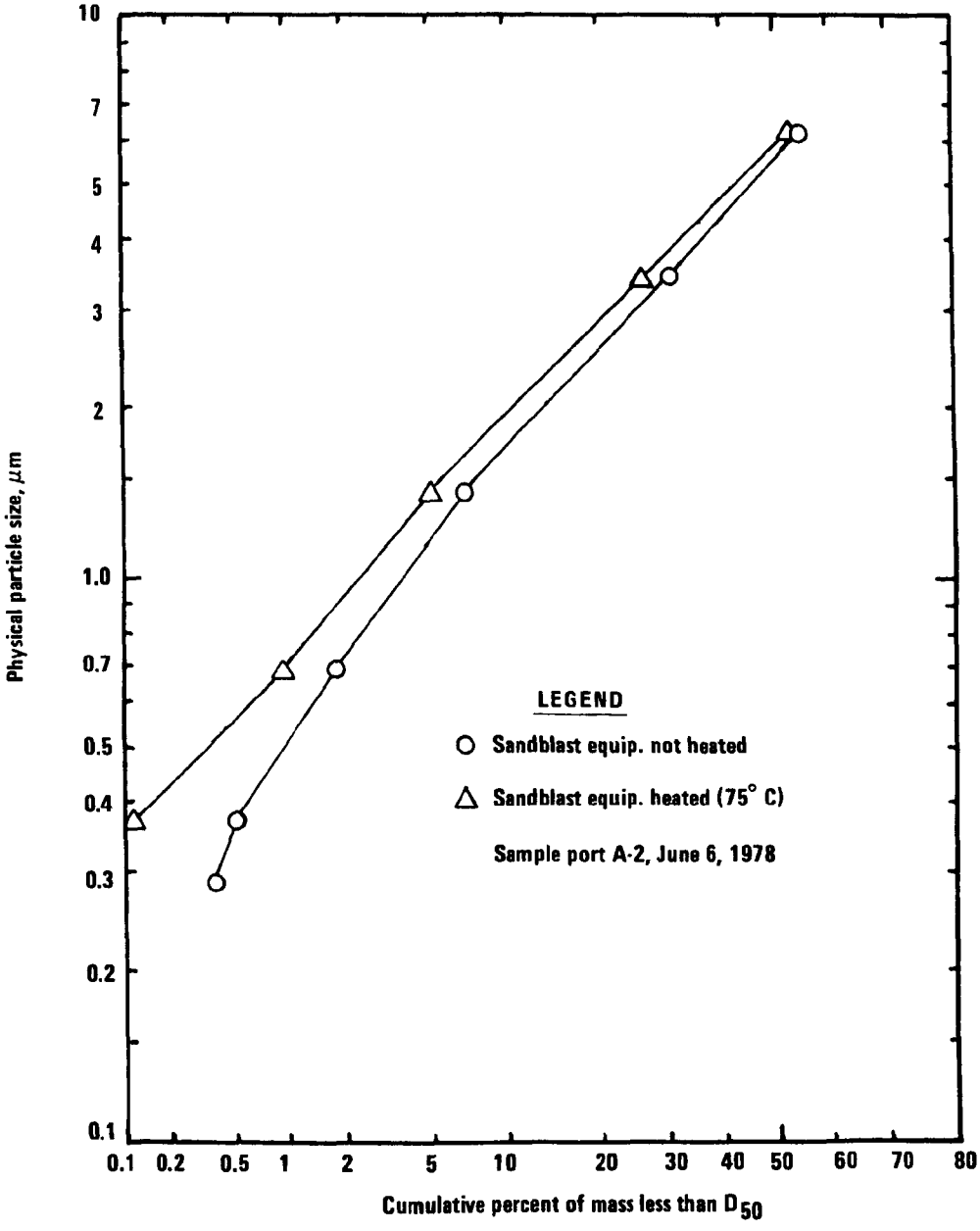

Figure 6.8 Effect of particle generation equipment temperature on size distribution, June 6, 1978.

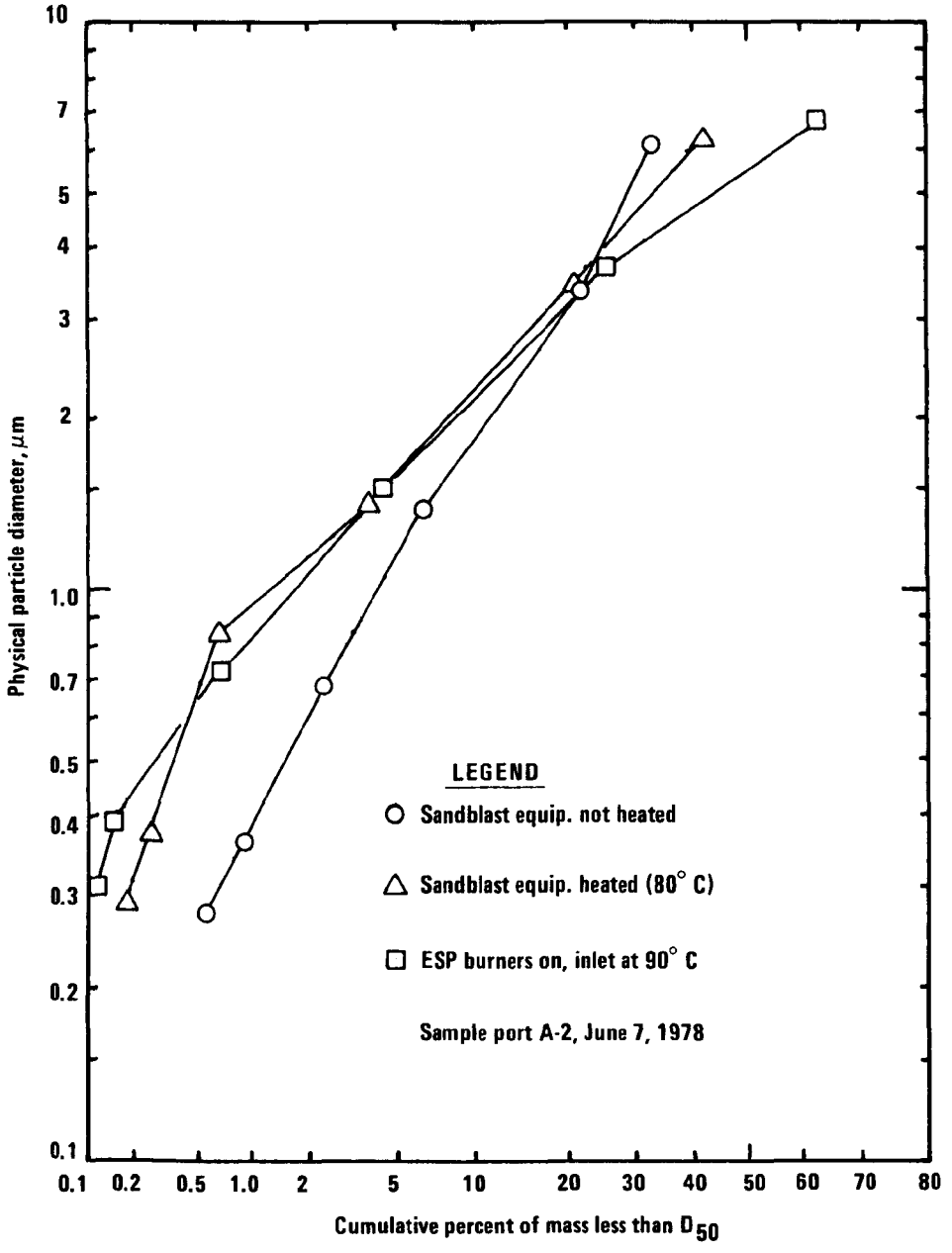

Figure 6.9 Effect of particle generation equipment temperature on size distribution, June 7, 1978.

7.0 HUMIDIFICATION RUNS

7.1 INTRODUCTION

A series of tests were run in September and October 1978 to investigate the effects of increased relative humidity on ESP performance. The humidity was controlled by steam injection as described below. The test series included 10 runs.

7.2 EXPERIMENTAL DESIGN

The operating parameters for the ESP during these tests are outlined below. Electrically, the ESP was operated at a voltage just below sparking, and the electrical data were recorded.

Gas Flow	:	28 m^3/min (1000 cfm)
Temperature	:	135 °C (275 °F)
Dust Injection	:	Flyash; by sandblast guns
Rapping	:	Section 1 rapped every 4.5 min Section 2 rapped every 10 min Sections 3 and 4 rapped once per 99 min program
Plate Spacing	:	23 cm (9 in.) all sections
Wires	:	23 cm (9 in.) spacing all sections, all tests except wire spacing of 7.6 cm (3 in.) in sections 3 and 4 from 8/30/78 to 9/18/78
Steam	:	378 kPa absolute when on
Humidity	:	Ambient ($\approx$2%) when steam off; 6-8% with steam on.

7.3 RESULTS

A summary of the data collected during the humidification runs is presented in Table 7.1. The collection efficiency of the ESP was definitely enhanced by the increased humidity of the carrier gas. The scatter in the data at low humidity led to a search for a stronger correlation. Figures 7.1 and 7.2 show that the average section 1 voltage during a run was a satisfactory independent variable. The correlation is very good for both exponential and power function fits, with the power function correlation being slightly better (r^2 of 0.974 to an r^2 of 0.971 for the exponential).

Particulate size distributions were determined by impactor for the inlet and outlet of the ESP, and the penetrations were calculated when possible, as presented in Figure 7.3.

Table 7.1. Summary of Humidification Runs

Date (1978)	Inlet Dust Loading, g/m^3	ESP Efficiency, %	ESP Penetration, %	Water Volume %	Mass Median Diameter, μm Inlet	Mass Median Diameter, μm Outlet	Section 1 Average Voltage
8/30	1.01	93.1	6.9	2.3	10.7	6.0	Not available
9/11	1.12	83.8	16.2	2.3	11.3	6.0	25.4
9/12	1.05	85.6	14.4	2.3	10.1	6.1	25.9
9/13	1.08	95.1	4.9	7.2	10.0	6.4	30.3
9/14	0.92	95.9	4.1	7.4	8.1	3.5	30.5
9/18	0.80	97.2	2.8	6.3	7.2	3.8	35.0
9/29	1.21	77.4	22.6	1.8	12.0	8.2	22.4
10/3	1.14	80.2	19.8	1.8	10.2	7.0	24.8
10/4	1.14	97.9	2.1	7.4	10.1	3.6	36.5
10/5	0.98	98.2	1.8	7.6	12.1	3.6	36.6

Plate and Wire Spacings: plate-to-plate--22.9 cm (9 in.); wire-to-wire all sections--22.9 cm (9 in.) for 9/29/78 to 10/5/78; sections 1 and 2--22.9 cm (9 in.), sections 3 and 4--7.6 cm (3 in.) 8/30/78 to 9/18/78

Temperature: 135°C (275°F)

Rapping Program: Section 1 every 4.5 min; section 2 every 10 min; sections 3 and 4 once per 100 min.

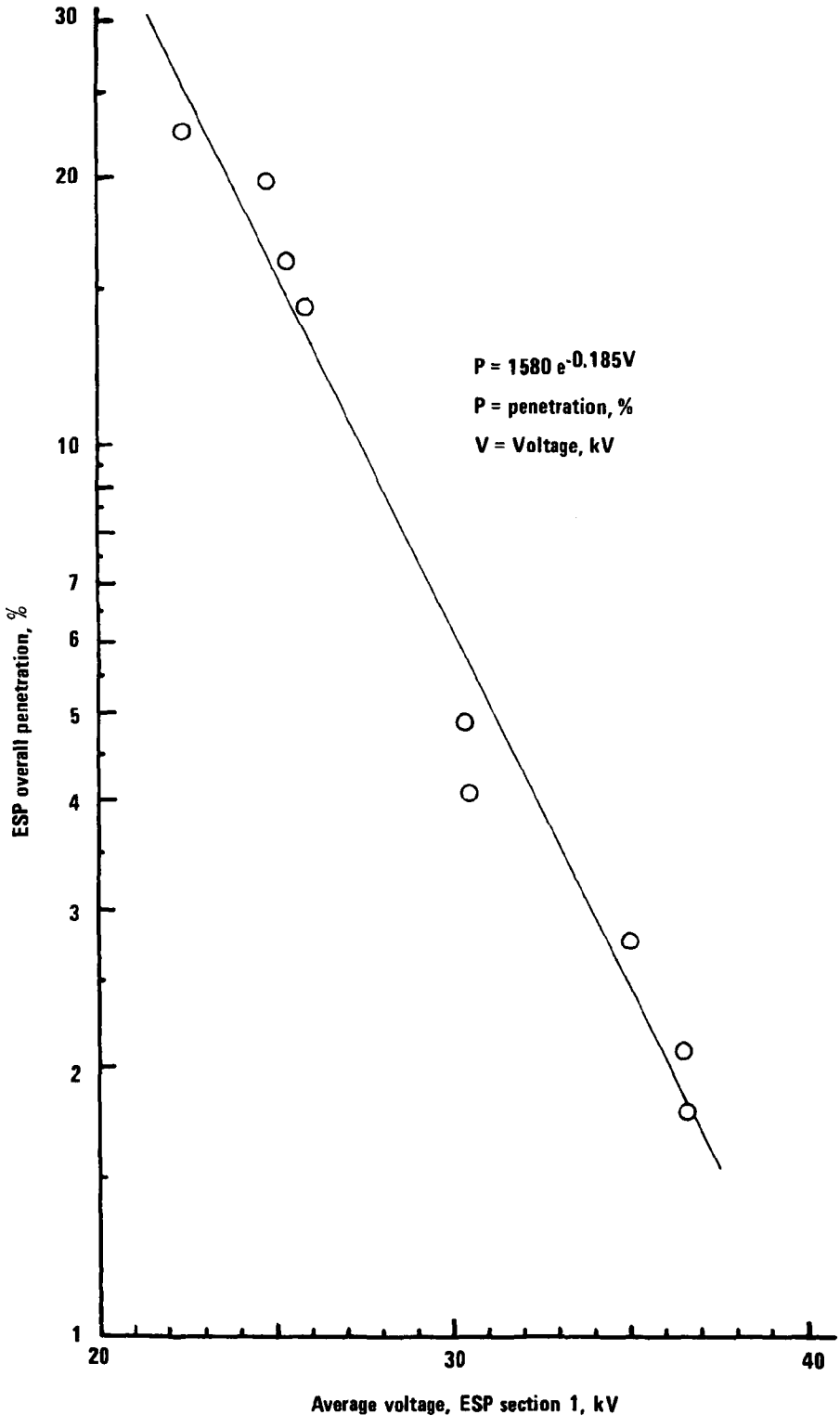

Figure 7.1 Correlation of voltage and penetration, exponential fit.

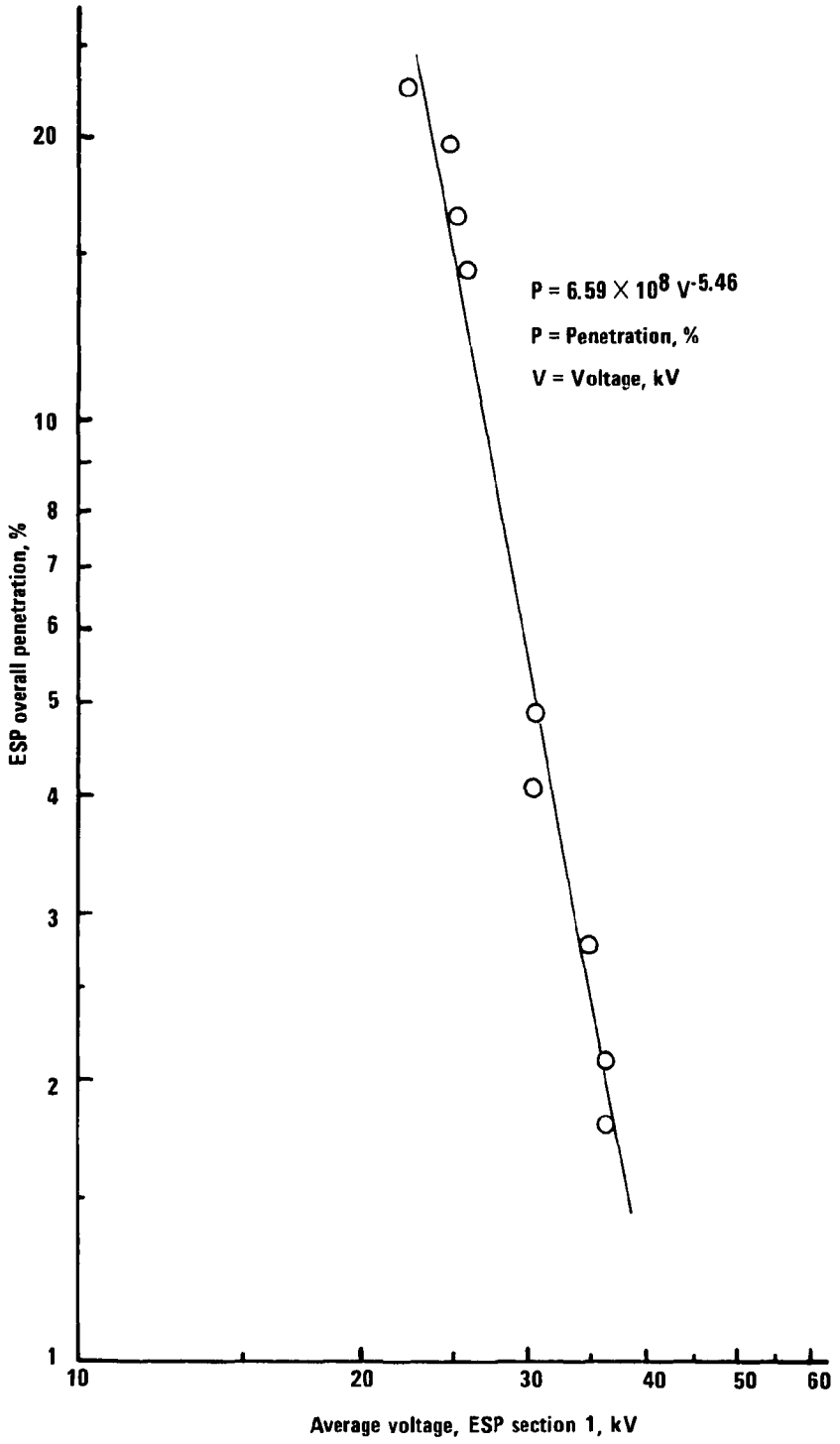

Figure 7.2 Correlation of voltage and penetration, power law fit.

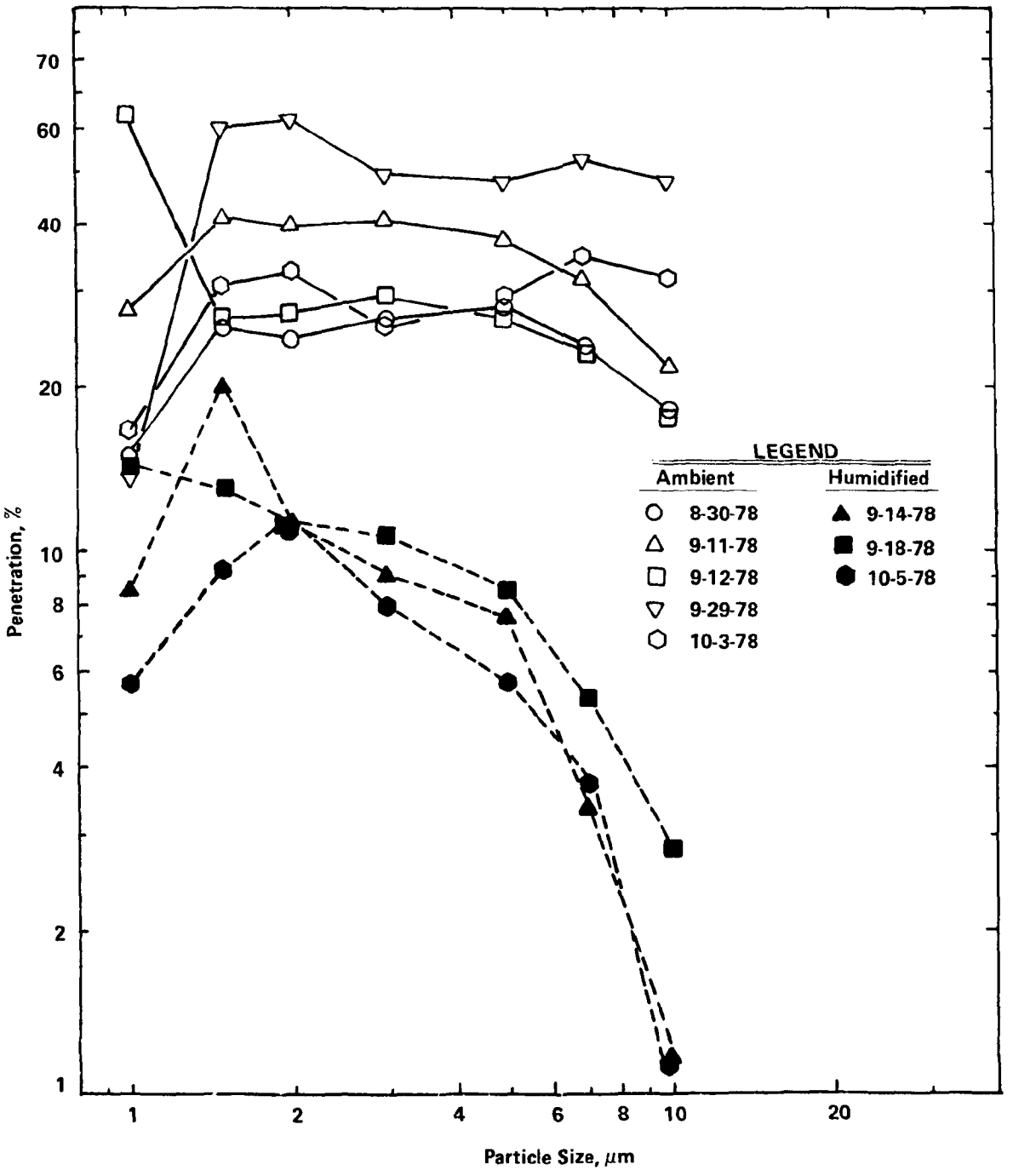

Figure 7.3 Penetrations for humidification runs.

Along with the normal automatic record of electrical data, VI curves for each section were obtained before and after the runs. A summary of these data is presented in Figure 7.4 for ESP section 1. These data were recorded directly from the ESP data bus on an X-Y recorder. The voltage was advanced manually. The detail presented in this plot is not available from an incremental VI plot. In every case, low humidity runs did not reach the voltage possible under high humidity conditions at equivalent current settings. The VI characteristics following a run were always less desirable than at the beginning of a run. The high humidity air was sufficient to improve the VI characteristics even before any dust had been collected.

7.4 CONCLUSIONS

The effect of the high humidity was apparently to improve the electrical characteristics of the dust, thereby allowing more intensive collection fields and higher efficiencies. The improvement in collection is a very strong function of voltage, showing that modest improvements in field strength can have a significant effect on efficiency.

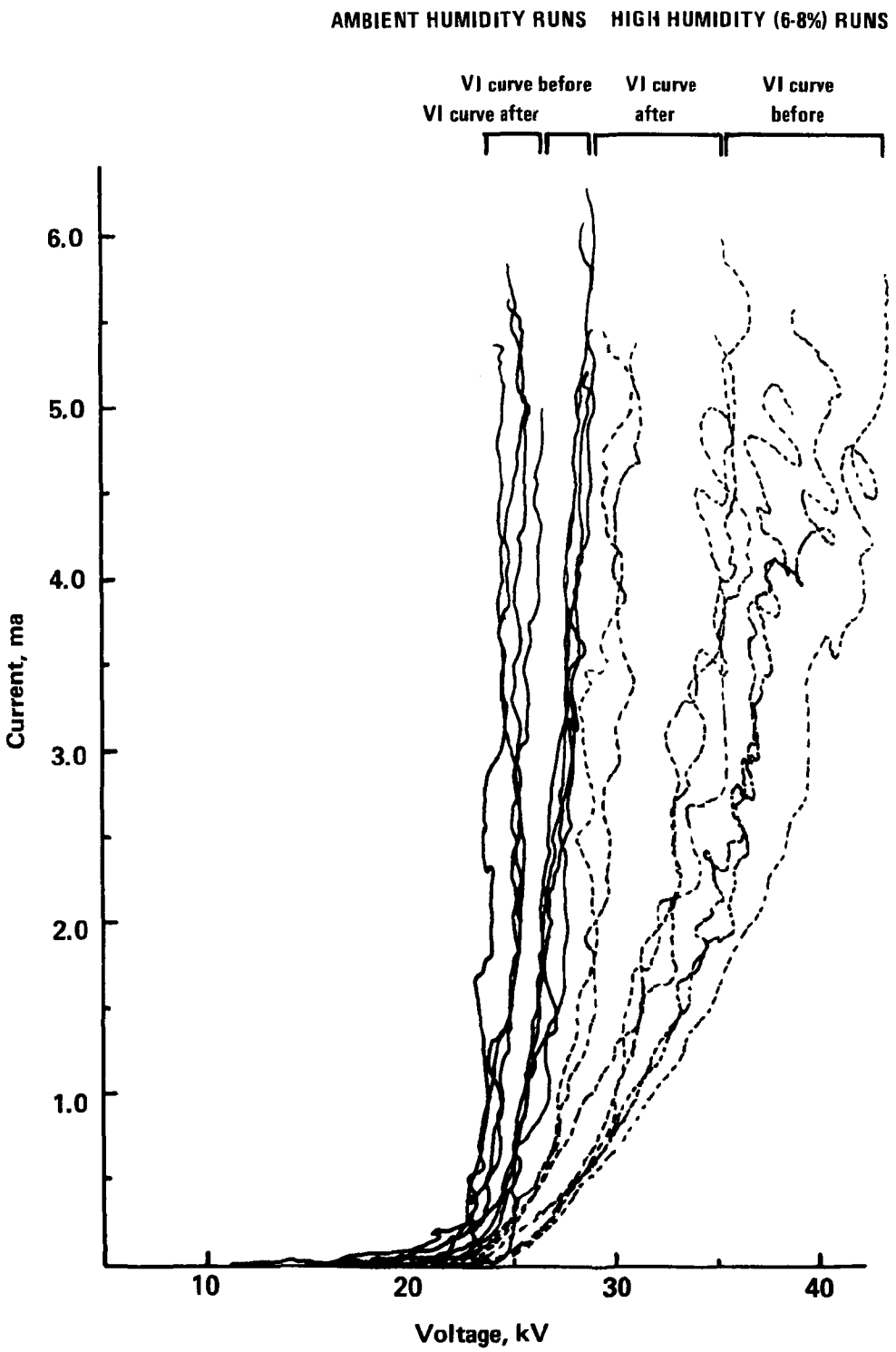

Figure 7.4 VI curves for ESP Section 1.

REFERENCES

1. Sparks, L.E., Cascade Impactor Data Reduction with SR-52 and TI-59 Programmable Calculators, EPA-600/7-78-226 (NTIS PB 290 710), November 1978.

2. Mercer, T.T. and R.G. Stafford, "Impaction from Round Sets," Ann. Occupational Hygiene. Vol 12, pp. 41-48, 1969.

3. Pontius, D.H., P.V. Bush, and L.E. Sparks, "A New Precharger for Two-stage Electrostatic Precipitation of High Resistivity Dust," Published in Symposium on the Transfer and Utilization of Particulate Control Technology: Volume I. Electrostatic Precipitators, EPA-600/7-79-044a (NTIS PB 295 226), pp. 285, February 1979.

TECHNICAL REPORT DATA
(Please read Instructions on the reverse before completing)

1. REPORT NO.	2.	3. RECIPIENT'S ACCESSION NO.
EPA-600/7-79-238		

4. TITLE AND SUBTITLE	5. REPORT DATE
EPA/IERL-RTP Pilot Electrostatic Precipitator--Selected Experiments, 1978	November 1979
	6. PERFORMING ORGANIZATION CODE
7. AUTHOR(S)	8. PERFORMING ORGANIZATION REPORT NO.
D.W. VanOsdell (RTI), L.E. Sparks, G.H. Ramsey, and B.E. Daniel	
9. PERFORMING ORGANIZATION NAME AND ADDRESS	10. PROGRAM ELEMENT NO.
See block 12.	EHE624A
	11. CONTRACT/GRANT NO.
	NA (Inhouse)
12. SPONSORING AGENCY NAME AND ADDRESS	13. TYPE OF REPORT AND PERIOD COVERED
EPA, Office of Research and Development **Industrial Environmental Research Laboratory** **Research Triangle Park, NC 27711**	Final; 6/78 - 6/79
	14. SPONSORING AGENCY CODE
	EPA/600/13

15. SUPPLEMENTARY NOTES IERL-RTP project officer is Leslie E. Sparks, Mail Drop 61, 919/541-2925.

16. ABSTRACT The report describes experiments with a pilot-scale electrostatic precipitator (ESP) at EPA/IERL-RTP. The ESP is a dedicated experimental tool, operated for experiments originated and designed both in-house and by EPA contractors. Five distinct test series, between March and October 1978, are described: precharger operation, ESP operating characteristics, reentrainment, parameter variation with position within ESP, and effects of humidity. The precharger test results were inconclusive; removal efficiency was 10-20% better with the precharger for most size ranges, but its operation was erratic. In the reentrainment test, sparking produced more and larger particulate than other reentrainment mechanisms. No size distribution change pattern was established. The study of flow, mass, and particle size as a function of sample probe position showed that parameter variations do exist; however, insufficient data was collected to fully establish the differences. In the study of the effects of humidity on collection efficiency, increased moisture had a strong impact on improved performance. Moisture lowered the particulate resistivity, allowing increased electrical fields. Efficiency correlated well with voltage in the form: P=6.59 x 10 to the 8th power x V to the -5.46 power where P=penetration, %, and V=voltage, kV. The correlation coefficient, r2, was 0.97.

17. KEY WORDS AND DOCUMENT ANALYSIS

a. DESCRIPTORS	b. IDENTIFIERS/OPEN ENDED TERMS	c. COSATI Field/Group
Pollution	Pollution Control	13B
Electrostatic Precipitators	Stationary Sources	13H
Tests	Precharging	14B
Humidity	Reentrainment	
	Sparking	

18. DISTRIBUTION STATEMENT	19. SECURITY CLASS *(This Report)*	21. NO. OF PAGES
Release to Public	**Unclassified**	61
	20. SECURITY CLASS *(This page)*	22. PRICE
	Unclassified	

EPA Form 2220-1 (9-73)